ESTIMATING THE SPATIAL DISTRIBUTION OF FIELD-APPLIED MUSHROOM COMPOST IN THE BRANDYWINE-CHRISTINA RIVER BASIN USING MULTISPECTRAL REMOTE SENSING

by

Kelsey A. Moxey

A thesis submitted to the Faculty of the University of Delaware in partial fulfillment of the requirements for the degree of Master of Science in Water Science and Policy

Summer 2016

ESTIMATING THE SPATIAL DISTRIBUTION OF FIELD-APPLIED MUSHROOM COMPOST IN THE BRANDYWINE-CHRISTINA RIVER BASIN USING MULTISPECTRAL REMOTE SENSING

by

Kelsey A. Moxey

Approved: _____
Luc Claessens, Ph.D
Professor in charge of thesis on behalf of the Advisory Committee

Approved: _____
Shreeram P. Inamdar, Ph.D.
Director of the Graduate Program in Water Science and Policy

Approved: _____
Mohsen Badiey, Ph.D.
Acting Dean of the College of Earth, Ocean, and Environment

Approved: _____
Ann L. Ardis, Ph.D.
Senior Vice Provost for Graduate and Professional Education

ACKNOWLEDGMENTS

I would like to extend my sincerest gratitude to my advisor, Dr. Luc Claessens for the support, guidance, and wisdom over the course of this research. This work would have not been possible if it were not for his mentorship. I would also like to thank my committee members, Dr. Gerald Kauffman and Dr. Byungyun Yang, for being a part of this journey and their positive support.

Also, I would like to thank Michael Zuk and Ben Drover from the Chester County Conservation District for their plethora of knowledge they had to share. Thanks are given to fellow master's student: Thomas Santangelo, and undergraduate student: Sandra Demberger for their contributions to this project.

Last but certainly not least, I extend an endless thank you to all of my incredible friends, family, and boyfriend for their unwavering emotional support throughout this entire journey. I certainly would not have come this far without them believing in me. Thank you to again to everyone who made this possible.

This work was partially funded by a grant of the Delaware Environmental Institute's Environmental Frontiers Grant Program, awarded to Dr. Luc Claessens.

TABLE OF CONTENTS

LIST OF TABLES

LIST OF FIGURES

ABSTRACT

The world's greatest concentration of mushroom farms is settled within the Brandywine-Christina River Basin in Chester County in southeastern Pennsylvania. This industry produces a nutrient-rich byproduct known as spent mushroom compost, which has been traditionally applied to local farm fields as an organic fertilizer and soil amendment. While mushroom compost has beneficial properties, the possible over-application to farm fields could potentially degrade stream water quality. The goal of this study was to estimate the spatial extent and intensity of field-applied mushroom compost. We applied a remote sensing approach using Landsat multispectral imagery. We utilized the soil line technique, using the red and near-infrared bands, to estimate differences in soil wetness as a result of increased soil organic matter content from mushroom compost. We validated soil wetness estimates by examining the spectral response of references sites. We performed a second independent validation analysis using expert knowledge from agricultural extension agents. Our results showed that the soil line based wetness index worked well. The spectral validation illustrated that compost changes the spectral response of soil because of changes in wetness. The independent expert validation analysis produced a strong significant correlation between our remotely-sensed wetness estimates and the empirical ratings of compost application intensities. Overall, the methodology produced realistic spatial distributions of field-applied compost application intensities across the study area. These spatial distributions will be used for follow-up studies to assess the effect of spent mushroom compost on stream water quality.

Chapter 1

INTRODUCTION

The world's greatest concentration of mushroom farms is settled within the Brandywine-Christina River Basin in Chester County in southeastern Pennsylvania. This agricultural industry produces a nutrient-rich byproduct known as spent mushroom compost, also referred to as "compost". Traditionally, compost has been applied to local farm fields as an organic fertilizer and soil amendment. It contains high organic matter and possesses moisture retention properties in contrast to other organic fertilizers (Fidanza et al., 2010; Lou et al., 2015). When compost is over applied to farm fields, it has potential to degrade stream water quality (Suess and Curtis, 2006; PADEP, 2012). In the Brandywine-Christina River Bain, locations of fields with applied compost are largely unknown. It is imperative to locate these fields in order to evaluate their effect on stream water quality.

This study is a part of a greater research effort to target watershed restoration efforts in the Brandywine-Christina River Basin. The goal of this study is to estimate the spatial extent and intensity of field-applied mushroom compost. Geospatial technologies, such as remote sensing, provide an avenue to identify the spatial extent of field-applied mushroom compost on a watershed scale. This is the first study that uses remote sensing to map field-applied compost from the field-scale to the watershed scale. In this study we applied a remote sensing approach using the soil line technique and used Landsat multispectral imagery, to calculate variation in soil wetness as an indicator of field-applied mushroom compost. We validated estimates of

field-applied mushroom compost using spectral and empirical data, and we examined estimates of field-applied mushroom compost from the field-scale to the watershed-scale.

This thesis is organized as follows. Chapter 2 introduces the study area, mushroom farming and general local water quality issues, and reviews remote sensing of soil organic matter. Chapter 3 describes our methodology. Chapter 4 presents the results and discussion, and Chapter 5 states the conclusions.

Chapter 2

BACKGROUND

2.1 Study Area: The White Clay Creek and Red Clay Creek Watersheds

The study area is located in the headwaters of the White Clay Creek and Red Clay Creek watersheds in the Brandywine-Christina River Basin. These two watersheds are located on the border of southern Chester County, Pennsylvania and New Castle County, Delaware (Figure 2.1). Collectively, the watersheds make up approximately 417 square kilometers, where 55 percent of the watersheds fall in the Pennsylvania, 45 percent falls in Delaware, and less than 1 percent falls in Maryland (Table 2.1). Their headwaters are situated in the Piedmont in Pennsylvania. The topography of this region consists of rounded hills with slopes varying from 15 to 20 percent, with irregular plains and narrow streams (PADEP, 2003). Soils are predominately well-drained, medium textured with underlying gneiss and schist. These headwater streams eventually flow south into Delaware, where they cross the fall line before their confluence with the Christina River (PADEP, 2003). The Christina River then empties into the Delaware Bay, a large estuary tucked in the Mid-Atlantic region of the United States. The region falls within a humid-subtropical climate that receives roughly 1.2 meters of precipitation annually.

We focused our study area to Chester County, Pennsylvania, where most mushroom farming operations are located. In both watersheds, land use consists of roughly one third forest, urban/suburban development, and agriculture respectively (University of Delaware Water Resources Agency, n.d. a; University of Delaware Water Resources Agency, n.d. b). Most of the urban/suburban areas are located in the southern portion of the watersheds (Figure 2.2), with high population densities

surrounding Newark, Delaware and the I-95 corridor. The northern portion of the watershed predominately consists of farming operations and agricultural fields (Figure 2.2). In the headwaters, there are lower population densities with smaller townships, including Kennett Square, New Garden, West Chester, and Avondale.

The White Clay Creek and Red Clay Creek watersheds are acknowledged for their federal and state importance, and local economic value. The White Clay Creek is federally recognized as a National Wild and Scenic River, which uses a watershed approach to protect its water quality. The White Clay Creek serves as a municipal drinking water supply for over thirty thousand people in Newark, Delaware and the surrounding area. In the Red Clay Creek, the state of Delaware recognizes a portion of the watershed as part of the Red Clay Valley Wild and Scenic Byway. This status helps preserve water quality for the area's ecological and cultural existence. The Red Clay Creek also has four surface water intakes and numerous private wells that supply drinking water for local residents (Chester County Water Resources Authority, 2002). For the combined watersheds, the groundwater and surface water is economically valued at approximately $565 million and provides approximately $249 million in ecosystem services (Cruz and Miller, 2014).

The headwaters of the White Clay Creek and Red Clay Creek watersheds possess great economic value from its diverse farming operations that rely on the water supply. Agriculture is the largest economic sector in Chester County, Pennsylvania and mushroom farming is the dominant activity (Table 2.2). The headwaters of these watersheds contain the greatest concentration of mushroom farms in the world, which accounts for roughly $412 million in product sales, and contributes a total of $2.17 billion to the local economy (Chester County Agricultural

Development Council, 2012c). Other agricultural activities such as dairy farming, nurseries, horse farming, and row crops, are scatted throughout the headwaters of these watersheds. Predominately corn, soybeans, and hay grow in the crop fields in these watersheds (Figure 2.3).

Water quality is an issue in the White Clay Creek and Red Clay Creek watersheds. Over 66 percent of the streams in White Clay Creek and 91 percent of streams in the Red Clay Creek are considered impaired (Chester County Water Resources Authority, 2002; Narvaez and Homsey, 2016). Several factors attribute to the degradation of water quality which include: bacteria, dissolved oxygen, nitrogen, phosphorus, zinc, and suspended sediments (Cruz and Miller, 2014; Narvaez and Homsey, 2016).

One persisting concern involves elevated nutrient concentrations, specifically nitrogen, in the local waterways (PADEP, 2003; Cruz and Miller, 2014; Narvaez and Homsey, 2016). The watersheds are located in one of the largest nitrogen hotspot in the eastern US (Figure 2.4), and degraded water quality has been attributed from both urbanization and agriculture operations in the forms of point sources and nonpoint sources (University of Delaware Water Resources Agency, n.d. c; United Stated Geological Survey, n.d.). Between the 1970's and 1990's, nitrate levels up to 3.2 milligrams per liter were found in the White Clay Creek and Red Clay Creek, which exceeded Delaware's standard for drinking water of 1 milligram per liter (United States Geological Survey, n.d.). In recent years, nitrate concentrations in these streams still remain above the 1 milligram per liter drinking standard (Cruz and Miller, 2014; Narvaez and Homsey, 2016).

In recent years, extensive watershed restoration efforts have been employed to reduce the contributions from point source and nonpoint source pollution in both urbanized and agricultural areas (Miller, 2014). A key stakeholder organization is the Brandywine-Christina Basin Clean Water Partnership, which has participation from federal, state, and local governments, non-profits, water purveyors, and academic institutions. This partnership was formed by the Delaware River Basin Commission.

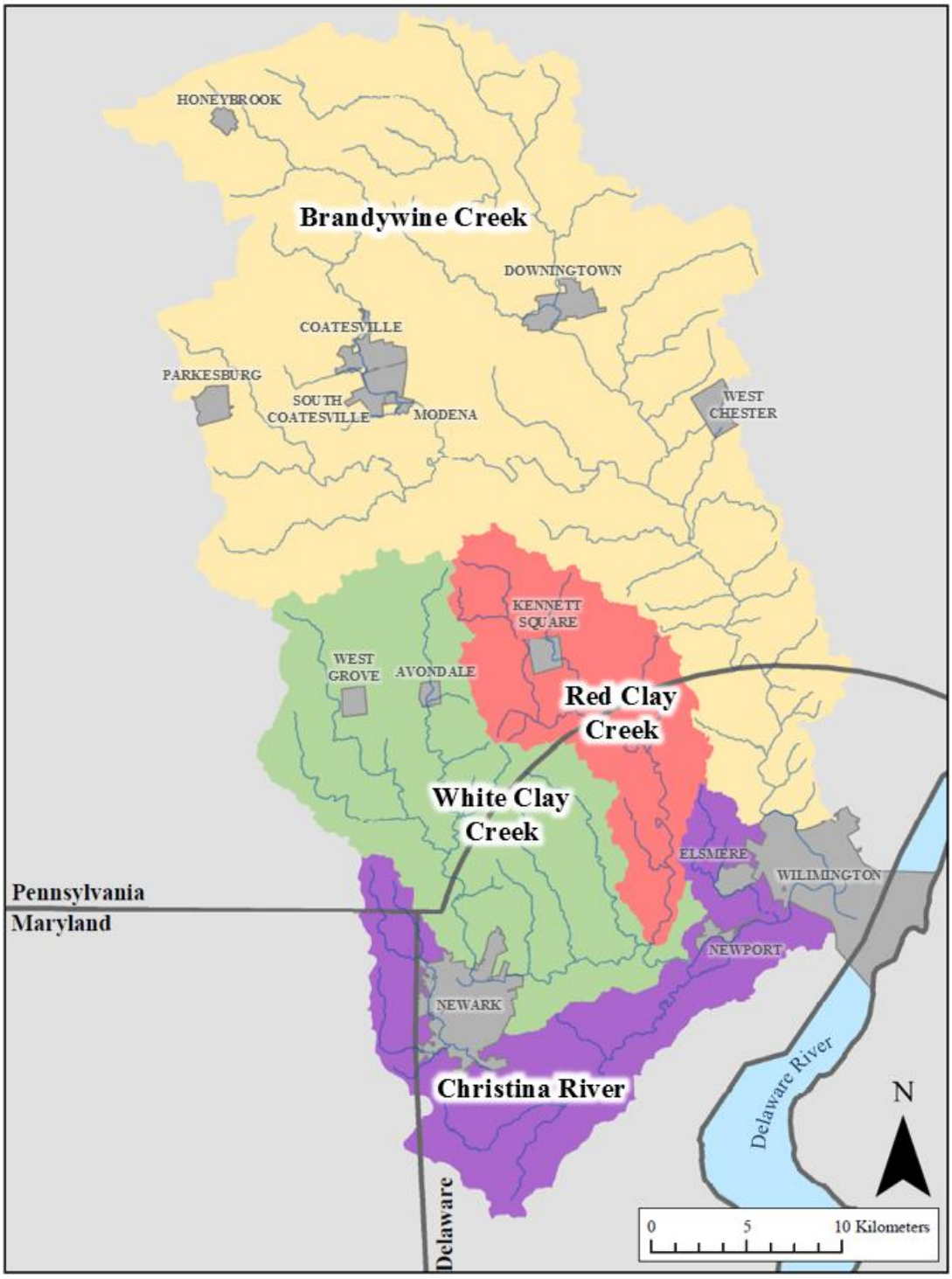

Figure 2.1: Reference map of the Brandywine-Christina River Basin.

Table 2.1: Watershed areas partitioned by state.

State	White Clay Creek (km^2)	Red Clay Creek (km^2)	Total watersheds (km^2)
Delaware	103	63	168
Maryland	2	0	0
Pennsylvania	125	77	202
Total area	230	140	417

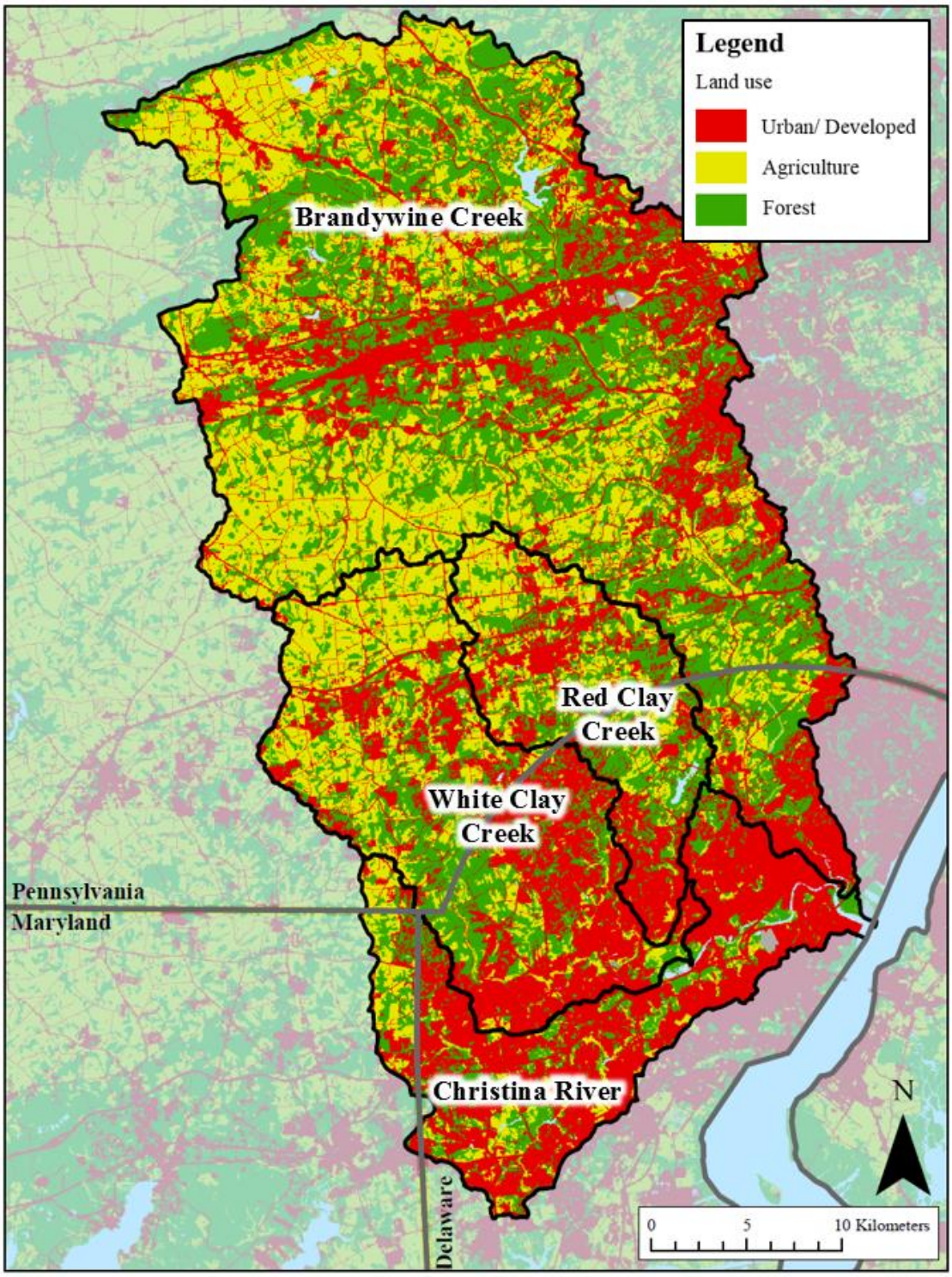

Figure 2.2: Land use of the Brandywine-Christina River Basin.

Table 2.2: Economic value and national/ state rank of agricultural operations in Chester County, Pennsylvania. Adapted from Chester County Agricultural Development Council (2012) and USDA National Agricultural Statistics Service (2012).

Industry	Economic value	Rank
Mushroom farming	$ 412 million	1st in United States
Nursey, greenhouse, and floriculture products	$ 79 million	1st in United States
Dairy farming	$ 73 million	6th in Pennsylvania
Row crops	$ 8.7 million	7th in Pennsylvania
Horse farming	$ 5.2 million	22nd in United States

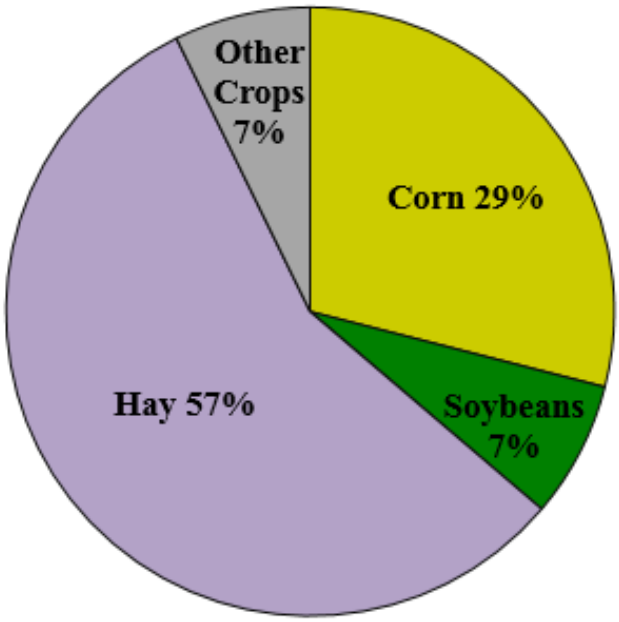

Figure 2.3: Dominant field crops in the White Clay Creek and Red Clay Creek watersheds.

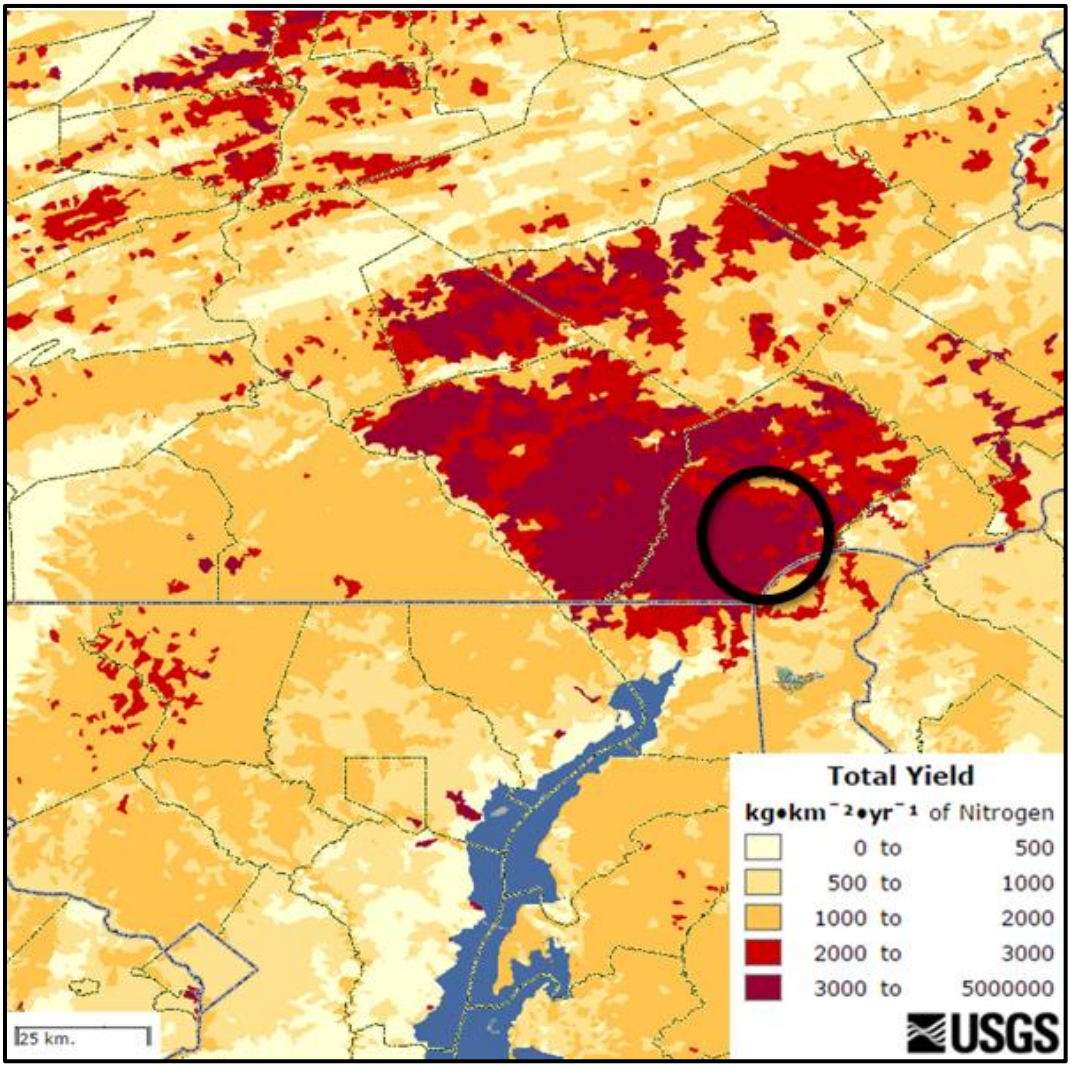

Figure 2.4: Estimates of total nitrogen yield in the Mid-Atlantic United States, from the 2002 Total Nitrogen Model for Northeast and Mid-Atlantic Regions, online SPARROW Decision Support System (http://water.usgs.gov/nawqa/sparrow/dss/) (USGS, 2002). Relative location of study area indicated by black circle.

2.2 Mushroom Production and Effect on Water Quality

2.2.1 History of mushroom production

For the past 125 years, high concentrations of mushroom farming operations labeled Kennett Square, Pennsylvania and its surrounding area, the "Mushroom Capitol of the World" (Flammini, 1999; McKay, 2008; Charles, 2012). During the late 1890's, mushroom production began with Quakers in Kennett Square, Pennsylvania importing mushroom spawn from Europe, specifically *Agaricus bisporus*, also referred as "white button mushrooms" (Charles, 2012). Mushrooms were first cultivated in greenhouses prior to building specialty houses to control climate conditions specifically for mushroom growing. With the advance of climate control technology in the 1920's and increased market demand, there was a large spike in mushroom production leading to a boom of mushroom farms (Flammini, 1999; McKay, 2008). This region provided suitable conditions for mushroom production because local horse farming were available to provide waster material for mushroom growing medium. By the 1930's over 500 mushroom houses, and over 350 mushroom growers surrounded a ten mile radius of Kennett Square, Pennsylvania (Flammini, 1999; McKay, 2008). During that time, this high concentration of mushroom farms produced over 85 percent of mushrooms in the United States (Flammini, 1999).

Mushroom farming still remains a large industry in this region, with roughly 60 mushroom growing operations in southern Chester County, that supply over 50 percent of the Unites States' mushrooms (McKay, 2008; Fidanza et al., 2010). Today's market demands caused smaller, less-efficient mushroom growing operations to be out-competed by larger growing facilities (Flammini, 1999; Charles, 2012). The larger farms require vast amounts of production materials, and therefore demand raw

materials to be imported into the watershed up to 160 kilometers away (Charles, 2012). Even though there are fewer farms today, mushroom production still dominates the headwaters of White Clay Creek and Red Clay Creek watersheds.

2.2.2 Mushroom production process

Growing mushrooms involves a multi-step process which includes: making mushroom substrate, growing mushrooms in houses, and managing spent mushroom compost. A single farming operation can manage one or more of these steps, which allows operations to become specialized in certain processes of the mushroom production process.

The process of mushroom farming begins at substrate production facilities, where raw materials are combined to create a growing medium for mushrooms, known as mushroom substrate. Making mushroom substrate involves composting large quantities of nutrient-rich materials (e.g. dairy/ horse manure, or chicken litter), organic carbon (e.g. hay, straw, or corn cobs), water, and other ingredients (Figure 2.5a). A comprehensive list of materials is listed in Table 2.3.

The raw materials are composted into mushroom substrate, a carbon-and nutrient-rich medium for growing mushrooms. This composting process of mushroom substrate usually occurs on large outdoor impervious surfaces, known as composting wharfs (PADEP, 2012). First, organic carbon materials (e.g., straw or hay), nutrient-rich materials (e.g., dairy/ horse manure, chicken litter) and water are mixed using custom machinery and placed in large piles, known as ricks (Figure 2.5b). These ricks are kept moist and turned over to stimulate aerobic activity, as temperature rises and ammonia accumulates in the substrate (Bayer, 2003). After 7- 16 days of composting the substrate, the substrate is pasteurized to kill any pests and unwanted microbes.

Leftover microbes continue converting the accumulated ammonia in the substrate into a viable, non-toxic form of nutrient for mushrooms to consume (Bayer, 2003). Once ammonia levels are low enough, the composting process is complete and the substrate is prepared for mushroom growing.

Mushroom substrate is then transported to growing houses, where it is used as a medium to grow mushrooms. Mushroom spawn, also referred as mycelia, are incorporated into the mushroom substrate. Once the mycelia fully colonize the substrate, it is placed into long trays, or beds, in climate-controlled growing houses (Figure 2.5c). Then, the trays of substrate are dressed with a casing layer, usually consisting of peat moss (PADEP, 2012). This casing stimulates mycelia into their reproductive state, prevents moisture loss, and provides a support structure for mushrooms to grow (Bayer, 2003). The mycelia emerge from the substrate and form small pins, or buttons, that grow large enough for harvesting. Pins double in size every 24 hours, and consume nutrients and water from the substrate (Figure 2.5d). Once the pins reach maturity, they are harvested. Pins continue to develop and grow in the substrate for 2 to 6 harvesting periods. After the final mushroom harvest, the entire house and substrate are pasteurized to destroy any pests or pathogens. The mushroom substrate is then removed from the growing house, and now becomes spent mushroom substrate. On an annual basis, over 1 million cubic meters of spent mushroom substrate are generated from mushroom houses (M. Zuk, personal communication, 2016).

The spent mushroom substrate is no longer considered viable for growing mushrooms due to its altered physical and chemical state, as it loses two thirds of its weight and volume after harvests (PADEP, 2012). The substrate is also high in organic

matter and contains elevated concentrations of nutrients and salts (Table 2.4). It is more economical to generate new substrate from raw materials than to adjust the physical and chemical state of spent mushroom substrate (Bayer, 2003).

Spent mushroom substrate is removed from mushroom growing facilities and transported off to other farming operations for other uses (see next). In the study area, a large proportion of the spent mushroom substrate is managed by mushroom brokers, who transport and further process the material. Most of the spent mushroom substrate is converted into mushroom compost, through passive or active composting. This process produces a highly valuable humus-like product that can be used for other practices (e.g., agriculture, gardening). In passive composting, spent compost is weathered in large piles for 6 months to 2 years, and stacked 1 to 1.5 meters high (Figure 2.5e). In active composting, the compost piles are frequently turned and the moisture content and temperature are regulated. The composting process leaches excess salts, and enhances microbial activity to alter its composition and texture (Bayer, 2003). Following the completion of this process, the mushroom compost is used for various applications, including fertilizer for crop fields and lawns, potting soil for horticulture and gardening, medium for green roofing material, and wetland construction for acid mine drainage (PADEP, 2012).

In this study we focus on the application of mushroom compost to local agricultural fields as an organic fertilizer and soil amendment (Figure 2.5f). The physical and chemical composition of compost allows nutrients to slowly release into the soil over a crop's growing season (PADEP, 2012). The slow-release properties in compost minimizes the potential for nutrient leaching into groundwater or surface water sources (Weust 1995; Weber et al., 1997). Compost also acts as an excellent soil

amendment due to its high organic matter content, which increases the water and nutrient holding capacity of the soils (Weber et al., 1997). Compost is uniformly applied to local farm fields at a rate between 1 to 13 centimeters, depending on a field's crop type (PADEP, 2012). Corn fields usually receive higher application rates than soybean and hay fields, due to corn's high nutrient demand (M. Zuk, personal communication, 2016). Because of the high transportation costs for hauling compost, these fields are generally located near composting facilities (Weber et al., 1997). The exact spatial distribution of these fields is largely unknown, which is the motivation for our study.

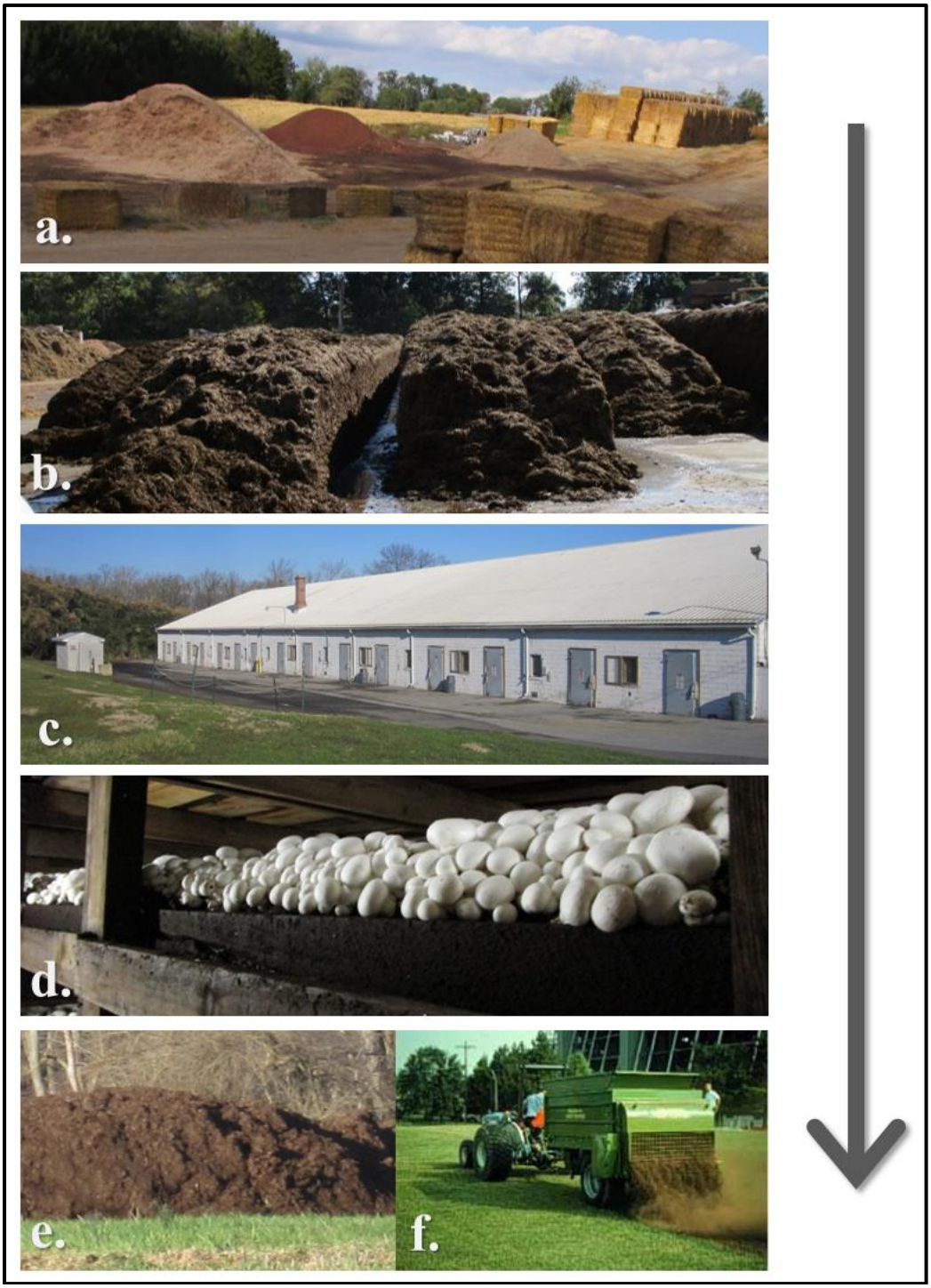

Figure 2.5: Mushroom production process (a-f). Photos courtesy of Kelsey Moxey (a, b, and d), Luc Claessens (c), Thomas Santangelo (e), and Landschoot and McNitt (n.d.) (f).

Table 2.3: Ingredients for mushroom substrate. Reprinted from PADEP (2012).

Ingredient	Rationale*				Typical Source	
	N[1]	C[2]	B[3]	O[4]		L[5]
MAIN INGREDIENTS						
Corncobs (whole, ground, crushed, pelletized)	X	X	X		Corn farm, corn sheller	
Hay	X	X	X		Hay farm	
Horse manure - straw bedded	X	X	X		Horse farm or track	X
Poultry litter/manure	X				Poultry farm	X
Straw		X	X		Grain farm	
SOME COMMON ADDITIONAL INGREDIENTS						
Ammonium nitrate	X				Fertilizer plant	X
Brewers grains (wet or dry)	X				Brewery	X
Corn fodder		X	X		Corn farm	
Feathers or feather meal	X				Poultry processor	
Grape pumice		X			Grape processor	
Ground wallboard				X	Soil conditioner supplier	
Gypsum				X	Gypsum rock	
Gypsum, synthetic				X	Soil conditioner supplier	
Hardwood tree leaves		X			Municipal leaf collection	
Lime				X	Soil conditioner supplier	
Mushroom stumps and culls			X		Mushroom farm	X
Seed - hulls		X			Seed processor	
Seed - meal	X				Seed processor	X
Seed - oil	X	X			Seed processor	
Shredded newspaper		X			Newspaper recycler	
Spent lime				X	Sugar processor	
Sugar cane (bagasse)		X	X		Sugar processor	
Sugar cane (pulp)		X			Sugar processor	
Urea	X				Fertilizer plant	X
Other substitute items may be found locally available						

* The above materials represent common ingredients used for the preparation of mushroom substrate, their function(s) in the substrate, potential for leaching, and typical sources. 1 = nitrogen, 2 = carbon, 3= bulk, 4 = other reasons, including flocculent or pH control, 5 = leachable.

Table 2.4: Chemical analysis of fresh spent compost on a wet volume basis. Reprinted from Fidanza et al., (2010).

			Range	
	Mean	SD	Minimum	Maximum
Parameter measured[z]			(lb/yard^3)[y]	
Bulk density	574.73	82.05	432.00	777.00
Solids	243.37	41.68	179.00	344.00
Moisture	331.47	71.70	209.00	469.00
Organic matter	146.73	17.67	119.00	199.00
Carbon	81.13	10.52	61.00	105.00
Total nitrogen	6.40	1.06	4.50	9.00
Organic nitrogen	6.19	1.07	4.30	8.80
Ammonium nitrogen (NH_4-N)	0.21	0.07	0.03	0.34
Phosphorus	1.67	0.41	0.90	2.95
Potassium	5.89	1.17	3.69	8.40
Calcium	13.17	3.31	6.71	20.28
Magnesium	2.01	0.61	0.99	3.53
Sulfur	4.91	1.12	3.12	7.72
Sodium	0.67	0.25	0.35	1.26
Aluminum	0.89	0.53	0.28	3.07
Iron	1.07	0.57	0.29	2.57
Manganese	0.12	0.07	0.04	0.29
Copper	0.03	0.01	0.02	0.08
Zinc	0.05	0.02	0.03	0.09

[z]Fresh mushroom compost samples (n = 30) were collected in 1-gal (3.8 L) containers and analyzed by the Agricultural Analytical Services Laboratory (Pennsylvania State University, University Park) from Jan. 2005 through Apr. 2005. Mushroom compost samples were analyzed "as is" when received at the laboratory for measurements on a wet volume basis. Actual phosphorus (P) was calculated from laboratory-measured P_2O_5 ($P = P_2O_5 \times 0.4365$), and actual potassium (K) was calculated from laboratory-measured K_2O ($K = K_2O \times 0.8301$).
[z]1 lb/yard^3 = 0.5933 kg·m^{-3}.

2.2.3 Water quality issues

The high concentration of mushroom production in this region has raised concerns related to the water quality impairments in the White Clay and Red Clay Creek watersheds (Chester County Water Resources Authority, 2002). In this section we review some of the potential concerns of water quality in the following stages of

mushroom production: substrate production, passive composting of spent substrate, and field-application of mushroom compost.

During the substrate production process, nutrients from agricultural waste products are concentrated in small areas to produce mushroom substrate. Under best management practices, any nutrient runoff from composting wharfs would be collected and reincorporated into the composting process (Weust, 1985). Nevertheless, streams near substrate production facilities are extremely susceptible to nutrient runoff. Results from extensive water quality sampling by Luc Claessens showed elevated nutrient concentrations downstream from substrate production facilities (Claessens, unpublished data).

Also the passive composting of the spent substrate into mushroom compost has the potential to affect water quality. The weathering in large compost piles can negatively impact groundwater and surface water quality (Figure 2.6a). Several studies have reported that nutrients can buildup in soils underlying compost piles (Kaplan et al., 1995; Guo et al., 2001a; Guo et al., 2001b; Guo et al., 2004). When nutrients build up in the soil over long periods of time, this is known as a legacy source where ground water can carry these nutrients into surface waters during base flow (Tesoriero et al., 2013).

The field application of the mushroom compost could also affect water quality. As previously mentioned, mushroom compost can be field-applied as a fertilizer or soil amendment, but it is uncertain what the effect is on water quality (Figure 2.6b). Weust et al. (1995) demonstrated that applying mushroom compost up to 90 kilograms per square meter in corn fields had minimal effects on surface water quality. Conversely, others claim the over application of mushroom compost can lead to water

quality impairments, especially when inorganic nitrogen is applied to supplement the slow-release nitrogen in the mushroom compost (Suess and Curtis, 2006; PADEP, 2012).

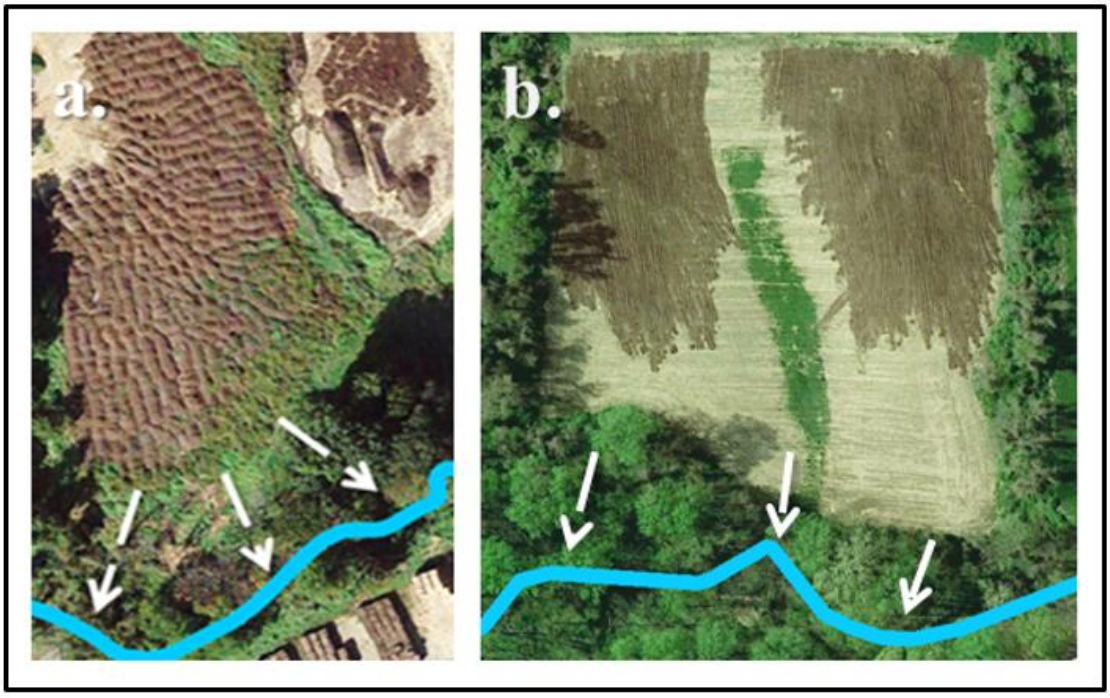

Figure 2.6: Mushroom compost can be located in close proximity to stream. These images show locations of: (a) piles of passive composting of spent mushroom substrate; (b) field-applied mushroom compost. The white arrows indicate the flow patterns to nearby streams (blue line).

2.3 Remote Sensing of Soil Organic Matter

2.3.1 Overview

Remote sensing has been valuable in the agricultural sector as an inexpensive method to monitor soil properties, such as soil moisture and soil organic matter (Ladoni et al., 2010b). Soil moisture is commonly used as an indicator of soil organic

matter, because organic matter increases the water holding capacity. The key concept behind remotely sensing soil moisture inherently relies on the decreased spectral reflectance across the electromagnetic spectrum, which is caused by the absorption properties of water (Baret et al., 1993; Ben Dor, 2001; Dematte et al., 2006; Croft et al., 2012). For a bare soil surface, a lower value for spectral reflectance suggests a higher soil moisture content, which infers a higher organic matter content. It is also important to consider other soil properties that could affect the spectral reflectance of soils, including soil texture, iron-oxide content, soil salinity, and surface roughness (Jensen, 2007).

Various remote sensing techniques have been developed across the electromagnetic spectrum to analyze soil moisture, and its related property of soil organic matter (Ben-Dor, 2001; Anderson and Croft, 2009; Ladoni et al., 2010b; Croft et al., 2012; Mulla, 2013). Ben-Dor (2001) argues hyperspectral imagery provides narrow band widths to distinguish soil properties, including soil organic matter. Other authors have utilized band combinations and indices in the visible, near infrared (NIR), and shortwave infrared wavelengths to identify soil moisture while normalizing atmospheric influences (Frazier and Cheng, 1989; Dupigny-Giroux and Lewis, 1999). Kauth and Thomas (1976) used bands in the visible to the short wave infrared wavelengths to develop the tasseled cap transformation which transfers spectral data into a three or four dimensional space, generating brightness, greenness, and wetness composite values.

2.3.2 The soil line concept

One useful technique for the remote sensing of soil moisture utilizes the concept of the soil line. This is the technique that we employed in this study. The soil

line is a linear relationship between the red and near infrared reflectance bands, first described by Richardson and Weigand (1977). A two-dimensional plot is constructed by the red and near infrared reflectance where pixels form an approximate triangle shape. Pixels towards the bottom of the triangle represent bare soil, which make up the soil line (Figure 2.7). Originally, the soil line concept was used to extract information on vegetation properties (Huete et al., 1992), but this technique can also be used to extract information on soil properties, particularly soil moisture and soil organic matter.

A pixel's position along the soil line in Red-NIR spectral space can determine its relative moisture content and extent of vegetative cover. Since moisture inherently decreases the spectral reflectance of a pixel, wet bare soils are positioned toward the lower portion of the soil line (Baret et al., 1993; Fox and Sabbagh 2002; Zhan et al., 2007; Yoshioka at el 2010; Gao et al., 2013) (Figure 2.7). Conversely, drier bare soils are positioned towards the upper portion of the soil line. When a pixel deviates from the soil line, biophysical properties such as vegetation greenness increase its NIR reflectance, which affects a pixel's soil signature (Richardson and Weigand, 1977; Jackson, 1983; Yoshioka et al., 2010).

Previous studies have used various transformations and empirical validation to demonstrate a relationship between the soil line and soil moisture/ soil organic matter. Caloz et al. (1988) developed the Normalized Soil Line Index to study the qualitative changes in surface soil moisture over time. Fox and Sabbagh (2002) developed a soil line transformation known as the Soil Line Euclidian Distance Technique, to determine soil sampling locations for varying degrees of organic matter. Dematte et al. (2006) related red and NIR spectral bands with empirical moisture measurements, and

concluded that the soil line technique can be used to interpret soil moisture from remotely sensed data. Recently, Ghulam et al. (2007) used the soil line technique to develop a Perpendicular Drought Index to monitor water stress in agricultural fields using a series of soil line transformations. Most of these studies only considered bare fields, unaffected by vegetation. To account for possible vegetation effects, other authors have recently developed methods which involve multifaceted steps (Gao et al., 2013; Taniguchi et al., 2016).

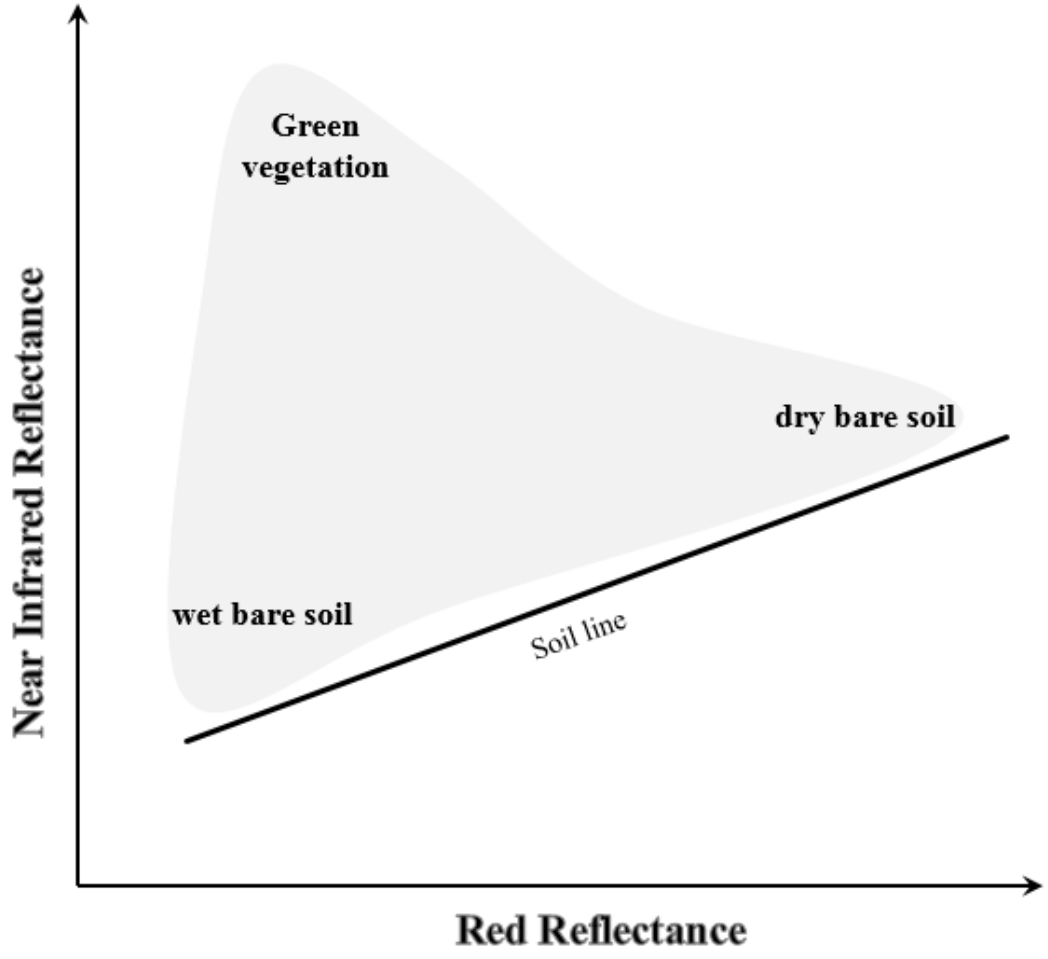

Figure 2.7: Soil line concept in Red-NIR spectral space.

Chapter 3

MATERIALS AND METHODS

3.1 Overview of Methodology

Compost increases the organic matter content of soils, which enhances soil moisture holding capacity and soil wetness. We estimated spatial patterns of field-applied mushroom compost by calculating a soil wetness index, using a remote sensing approach and Landsat multispectral imagery. The soil wetness index is calculated using a simple geometric transformation in Red-NIR spectral space, using the soil-line technique (Figure 3.1). We rely on the decreased spectral reflectance of moist soils to detect compost application. We used equations from basic soil line transformations to calculate a pixel's distance from the soil line, and then statistically normalized the values to create a soil wetness index. We validated the soil wetness index estimates by comparing three distinct types of reference sites: "compost piles", "fields with compost", and "fields without compost". As part of this spectral validation, we also examined how mushroom compost affects the spectral response over a growing season. We then performed a second, independent validation analysis with expert knowledge from agricultural extension agents. After validation, we produced maps of soil wetness index estimates for the entire study area. We examined the maps across spatial scales, from the field scale to the larger watershed scale.

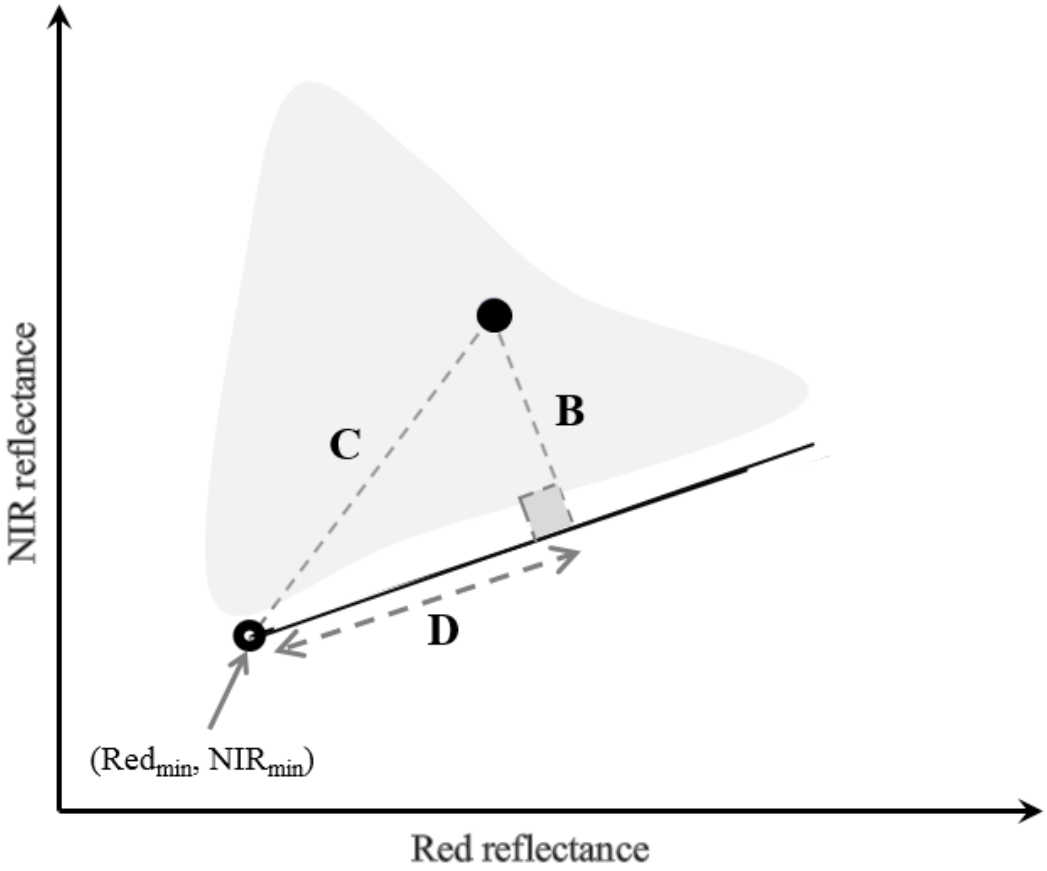

Figure 3.1: Conceptual model of wetness index calculations using the soil-line technique.

3.2 Materials

3.2.1 Satellite imagery

We used Landsat 5 Thematic Mapper data, which has been successfully used in the past to estimate soil organic matter and wetness (Kauth and Thomas 1976; Frazier and Cheng, 1989; Fox and Sabbagh 2002; Yoshioka et al. 2010; Xu and Guo, 2013). A key benefit of Landsat data is its temporal resolution (16 day intervals).

Landsat 5 has a spatial resolution of 30 meters and has 7 spectral bands ranging from visible to the thermal infrared (Table 3.1).

We selected the best Landsat scene using a set of criteria. First, agricultural fields needed to be bare for the sensor to capture an accurate spectral reflectance of bare soil, because vegetation hampers the spectral response (Muller and Decamps, 2000; Zhan et al., 2007; Ladoni et al., 2010b). Second, agricultural fields had to be low in antecedent soil moisture (Ladoni et al., 2010a) with minimal precipitation days before data acquisition (Scharf et al., 2002), in order to capture distinct differences in soil wetness. Since antecedent soil moisture conditions vary on seasonal and daily scales, it was important to select a scene during the driest time of the year outside the growing season (Dupingy- Giroux et al., 1999).

Based on these criteria we selected a scene from May 11, 2011, as explained below. To determine antecedent soil moisture conditions, we examined precipitation and soil moisture data from a local weather station, located in Kennett Square, Pennsylvania. The weather station is operated by the Delaware Environmental Observing System (DEOS). We first examined monthly average soil moisture and total precipitation between 2009 and 2014. Soil moisture was typically lower in the spring months before the growing season (Figure 3.2). We then evaluated scenes from Landsat 5 and Landsat 8 in the spring from each year, by examining daily precipitation and soil moisture data, and possible cloud interference. Imagery from Landsat 7 was not considered because the study area fell within a data gap from the scan line corrector failure. Based on these analyses we selected a Landsat scene from May 2011, because it had relatively low soil moisture, the least amount of rainfall prior to

scene acquisition, and minimal cloud interference. In addition, more cloud-free scenes were available throughout the year of 2011 for the temporal analysis (Figure 3.3).

We acquired preprocessed surface reflectance Landsat data from the United States Geological Survey website (https://gdg.sc.egov.usda.gov). All the images were previously geometrically corrected to World Geodetic System 1984 Universal Transverse Mercator, zone 18 north and converted to surface reflectance in 16 bit format. We clipped the data to the study area and extracted larger clouds with the cfmask cloud mask layer contained in the Landsat Surface Reflectance Data Product (USGS, 2015b).

Apart from Landsat data, we also used other sources of remote sensing data. For a preliminary analysis (Appendix A.1) we worked with high resolution multi-spectral aerial imagery from 2013 provided by the National Agricultural Imagery Program (NAIP), administered by the United States Department of Agriculture. NAIP collects imagery with four spectral bands at one meter spatial resolution. The four bands include the visible (red, green, blue) and NIR spectra. NAIP images are typically acquired once or twice a year during the agricultural growing seasons (USDA, n.d.). Because soils are generally covered by vegetation then, the imagery is not well suited to remotely sense soil properties. This was also confirmed in our preliminary analysis (Appendix A.1).

Table 3.1: Landsat 5 spectral bands and resolution. Adapted from USGS (2015a).

Bands	Description	Wavelength (micrometers)	Resolution (meters)
1	Blue	0.45-0.52	30
2	Green	0.52-0.60	30
3	Red	0.63-0.69	30
4	Near Infrared	0.76-0.90	30
5	Short-wave Infrared	1.55-1.75	30
6	Thermal Infrared	10.42-12.50	120 (resampled to 30)
7	Short-wave Infrared	2.08-2.35	30

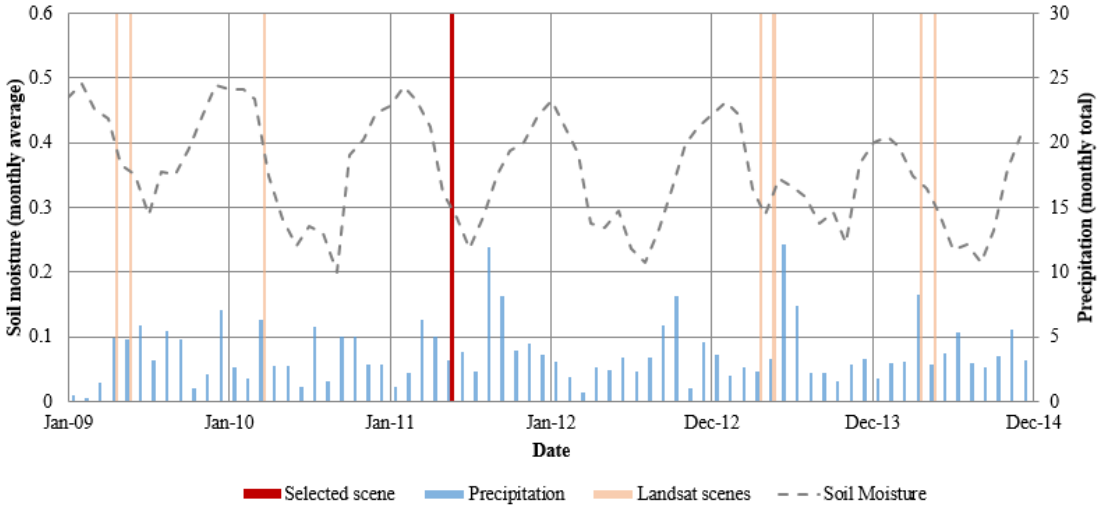

Figure 3.2: 2009-2014 monthly averaged soil moisture and total precipitation showing cloud-free Landsat scenes during the early spring growing season.

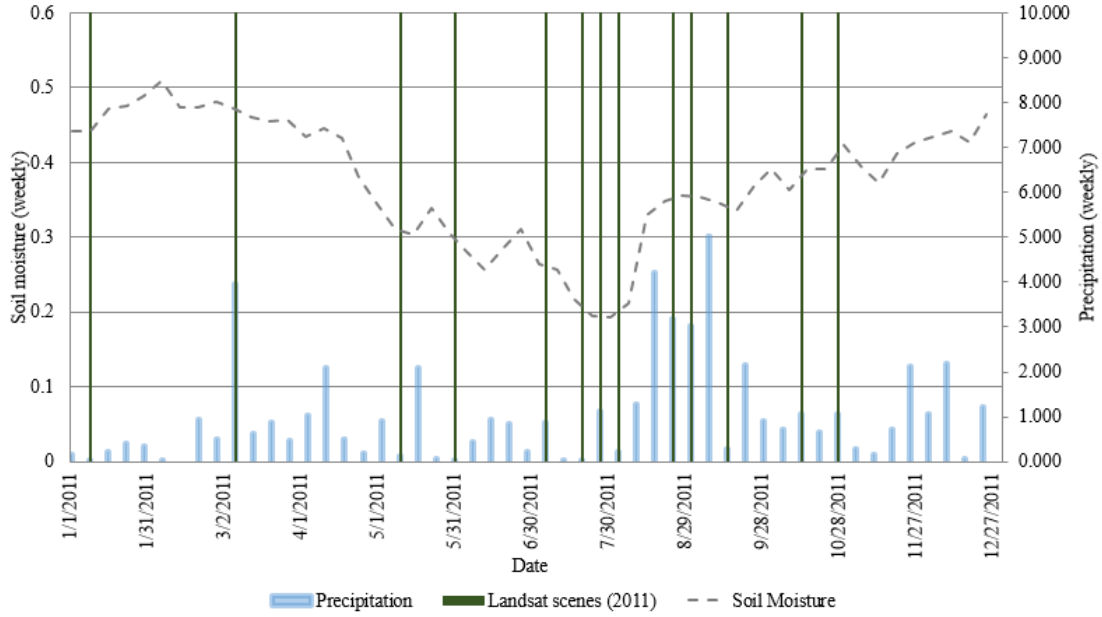

Figure 3.3: 2011 weekly averaged soil moisture and total precipitation, showing all cloud-free Landsat scenes over the course of the year.

3.2.2 Land use and soil type

We restricted our analysis to agricultural fields that have predominantly bare soils. To select these fields, we first extracted areas under agricultural land-use using a high resolution land use/land cover dataset developed by Chester County, Pennsylvania in 2005. Because land use change was relatively minor between 2005 and 2011, the land use data was considered accurate. Next, we restricted the analysis to agricultural fields that have bare soil. To do this, we utilized a coarse resolution (30 meter) Cropland Data Layer (CDL) from 2011, created by the National Agricultural Statistics Service (USDA, 2012). The CDL layer uses a combination of remote sensing and ground-truth observations to accurately assess different types of crop cover. This segregation of cropland types ensured we selected pixels that were only representative of bare soils.

We also examined the effect of soil type on the spectral response of soil moisture. Soil type has been known to affect the slope and y-intercept of the soil line, which can cause different spectral responses when detecting changes in soil moisture (Baret, 1983). In preliminary analysis we determined that variation in soil type did not affect the soil lines for the different cropland types (Appendix A.2). Therefore, we did not consider soil type, and segregated by cropland type only.

3.3 Soil Wetness Index

3.3.1 Soil line

We calculated the soil line using the (Red, NIR_{min}) method (Fox et al., 2004; Stabile and Searcy, 2009; Xu and Guo, 2013). First, we manually removed pixels affected by small clouds and their shadows, which the Landsat cloud-mask (cfmask) was unable to detect. We selected these suspect pixels by plotting them in Red-NIR

spectral space, and examining all the pixels that fell below and to the left of the dense pixel cluster in the spectral plot. We used higher resolution imagery to examine how land use affected these pixel's spectral response, and if a pixel showed an atypical spectral response from its land use, it was removed. After removing these suspect pixels we calculated the soil line using a standard technique, for which we calculated the minimum NIR reflectance value for each Red reflectance bin, followed by linear regression. The slope and y-intercept of the soil line were used in the wetness calculations.

3.3.2 Distance along the soil line

We calculated a pixel's distance along the soil line to derive its relative moisture content. The distance along the soil line refers to the length between a pixel and the minimum, left-most pixel on the soil line. The minimum, left-most pixel on the soil line represents the darkest soil, suggesting it has the highest soil moisture and organic matter of all fields in the study area (Fox and Sabbagh, 2002). We calculated each pixel's distance along the soil line using simple triangular geometric relationships in spectral space (Figure 2.1). The perpendicular distance from the soil line (side B in Figure 2.1) was calculated using the Perpendicular Vegetation Index (PVI) (Richard and Weigand, 1977), using the equation:

$$B = \frac{NIR-(a*Red)-b}{\sqrt{a^2+1}} \quad [1]$$

where: *NIR* and *Red* are the values for a given point in spectral space, *a* is the slope of the soil line, and *b* is the y-intercept of the soil line. The hypotenuse of the right triangle (Side C in Figure 2.1) was calculated using the Soil Line Euclidian Distance Index (SLED) (Fox and Sabbagh, 2002), using the equation:

$$C = \sqrt{(NIR - NIR_{min})^2 + (Red - Red_{min})^2} \quad [2]$$

where: NIR_{min} and Red_{min} are the reflectance values for the empirically derived minimum point along the soil line. This represents the wettest bare soil in the study area (Fox and Sabbagh, 2002; Ladoni et al., 2010b). The pixel's distance along the soil line (D) is calculated using Pythagoras' Theorem:

$$D = \sqrt{C^2 - B^2} \quad [3]$$

The calculations are combined in this following equation:

$$D = \sqrt{((NIR - NIR_{min})^2 + (Red - Red_{min})^2) - \left(\frac{NIR - (a * Red) - b}{\sqrt{a^2 + 1}}\right)^2} \quad [4]$$

3.3.3 Statistical normalization of distance values

The distance along the soil line (*D*) was corrected to account for outliers at either end of the soil line through a statistical normalization procedure. First, we extracted data points that only represent bare soil, falling within the 95 percent confidence interval of the fitted soil line. We then sorted the bare soil pixels' calculated distances to determine the 2.5 and 97.5 percentile distances, which we set as the minimum and maximum distance values for the normalization procedure. We normalized the distance values of all the pixels in the scene, with a final value ranging between 0 and 1, using the following equation:

$$D' = \frac{(D - D_{2.5})}{(D_{97.5} - D_{2.5})} \quad [5]$$

where: *D'* is the normalized distance along the soil line, and $D_{2.5}$ and $D_{97.5}$ are the 2.5 and 97.5 percentiles of distance along the soil line, respectively.

Distance values prior to normalization (*D*) that fell below the 2.5 percentile or above the 97.5 percentile, were set to zero or one, respectively. The model output

generated a raster of normalized distance values between 0 and 1, which represent degrees of wetness indicative of mushroom compost.

3.4 Validation Analysis

3.4.1 Single-scene spectral validation

To evaluate the predictive capability of our method, we first performed a single-scene validation analysis. We validated the wetness estimates using three sets of distinct types of reference sites that represent different degrees of wetness in terms of mushroom compost application: “compost piles”, “fields with compost”, and “fields without compost”. “Compost piles” are specific areas in farm operations where farmers stacked spent mushroom compost 1-1.5 meters high for passive weathering. The second set of reference sites are “fields with compost”. These fields had mushroom compost incorporated into their soils, but not as intensely as in the “compost piles”. The third set of reference sites are “fields without compost”. Those fields did not receive mushroom compost, and we would expect the soils to retain less moisture and dry out more quickly.

We carefully selected these reference sites by using a variety of data sets (Table 3.2). We selected “compost piles” and “fields with compost” by using a dataset of known farm parcels that produce substrate or manage compost; these farm parcels have a registered Mushroom Farm Nutrient Management Plan with the Chester County Conservation District. We selected “fields without compost” by focusing on agricultural fields located away from these known farm parcels. To select the reference sites we examined land-use history, using temporal sequences of high resolution aerial imagery using Google Earth, NAIP, and ChescoViews (Table 3.2).

Furthermore, we compared the Landsat pixels against the higher resolution imagery, to ensure proper representation of land use for each reference site.

For each reference type and vegetation combination, we selected six to eight different reference sites. Within these targeted reference sites, we carefully chose individual pixels that were considered true reference pixels and which were not affected by other land uses surrounding the pixels (Souza et al., 2005). After selecting the pixels for each reference site, we calculated the average value for Red and NIR spectral reflectance, and plotted the values in Red-NIR spectral space.

Table 3.2: Data used for reference site selection.

Data	Data type	Viewer	Source	Purpose
Known mushroom compost farms	parcel	ArcMap	Chester County Conservation District	identified known areas of compost piles and fields with compost
High resolution 1 meter imagery (2010 & 2013)	orthophoto	ArcMap	NAIP-USDA	visually inspected fields with and without compost
Historical images (1992-2015)	aerial photographs	Google Earth	Google Earth	objectively verified past land use and land cover of potential reference sites
High resolution imagery (2008, 2010, & 2014)	aerial photographs	Chesco Views R3.1	Chesco Views	visually inspected fields with and without compost

3.4.2 Multi-scene temporal spectral validation

We also conducted a multi-scene, temporal spectral validation analysis of the reference sites, by examining the change in spectral reflectance over the course of one year. To do this temporal analysis, we acquired multiple Landsat scenes for 2011 (Table 3.3). For each of the scenes we extracted the average spectral reflectance for

each reference site. For some scenes, we omitted certain sites in case of cloud interference or other potential sources of error. For each scene, we averaged the spectral values for the three main reference types, and plotted their temporal sequences in Red-NIR spectral space.

Table 3.3: Landsat scenes used in temporal analysis.

Date	Scene ID	Cloud cover
03/08/2011	LT50140322011067GNC01	0.4%
05/11/2011	LT50140322011131GNC02	2.8%
07/21/2011	LT50150322011202EDC00	4.4%
10/25/2011	LT50150322011298EDC00	0.2%

Note: Cloud cover value is for the extent of the study area.

3.4.3 Empirical validation using expert knowledge

We also performed an independent, empirical validation analysis of the wetness index/compost application estimates, using expert knowledge. We worked with two agricultural extension agents of the Chester County Conservation District, who have expert knowledge of farming operations in the study area. As described below, these experts rated the intensity of compost application for multiple sites across the study area. We then compared these empirical, expert ratings of compost application against our remote-sensing based wetness index values.

We selected sites across the entire study area, covering the full range of compost intensity values. We constrained the validation to parcels with a minimum

size of 4 hectares, and with wetness index values for at least 20% of the parcel. For each parcel, we calculated the average value for wetness index, and then grouped all the parcels into 5 classes (Table 3.4). Next, to obtain an unbiased and equal representation of validation sites across these classes, we applied a stratified random sampling approach, using the Sampling Design Tool for ArcGIS (Buja and Menza, 2013). The selection process of the validation sites focused on those regions of the study area where the agricultural extension agents were most familiar. We selected a total of 72 expert validation sites, with a fairly equal representation across the 5 wetness classes (Table 3.4).

The experts rated the compost application intensity of each site, on a scale from 1 to 5 (Table 3.4). We used Google Earth with standard aerial imagery, including historical imagery. The rating by the experts was done blindly, without knowledge of the corresponding wetness value. If the experts were unsure of a site's compost application intensity, we later excluded that site from statistical analysis. After the expert rating, we performed statistical correlation analysis. To reduce the effect of outliers, we used the median value of modeled wetness index for each expert compost rating class.

Table 3.4: Expert validation analysis structure.

Wetness index class	Compost intensity rating	Site count
0.00 - 0.20	1- Low to no compost	6
0.21 - 0.40	2- Medium to low	8
0.41 - 0.60	3- Medium	10
0.61 - 0.80	4- Medium high	10
0.81 - 1.00	5- High amount of compost	8

3.5 Mapping Wetness

After validation, we mapped soil wetness index values to examine the spatial extent and intensity of compost application across the study area. We interpreted patterns of wetness index values inside passive composting operations, surrounding passive composting operations, between adjacent crop fields, and on a watershed scale. First, we examined wetness patterns within passive composting operations. For these operations, we selected specific areas where compost was applied to examine its average spectral response. We interpreted the overall wetness patterns in each of the operations using Zonal Statistics. We also related the wetness index values in these operations to underlying land cover using historical imagery. Next, we interpreted patterns surrounding the watersheds using historical imagery. Then, we examined patterns between farm fields. Finally, we analyzed patterns on a watershed-scale to determine where compost is generally applied in the watershed and confirmed these observations with local agricultural extension agents.

Chapter 4

RESULTS AND DISCUSSION

4.1 Red-NIR Spectral Space

In Red-NIR spectral space, corn and soybeans formed typical triangle shapes (Figure 4.1a-b; Figure 4.2). Most of the pixels concentrated toward the bottom of the triangle resembling bare soil, so vegetation effects are relatively minimal. Pixels in the upper left corner of the corn and soybean spectral plots were considered outliers. It is possible a different type of crop was cultivated on these fields at the start of the growing season (e.g. cover crops).

Pixels in hay fields were positioned differently in Red-NIR spectral space. The pixels were clustered in the upper left corner in spectral space, which suggests that vegetation dominates hay fields' spectral responses (Figure 4.1c). Because the soil line method used in this study requires minimal vegetation interference, we therefore excluded hay fields from further analysis.

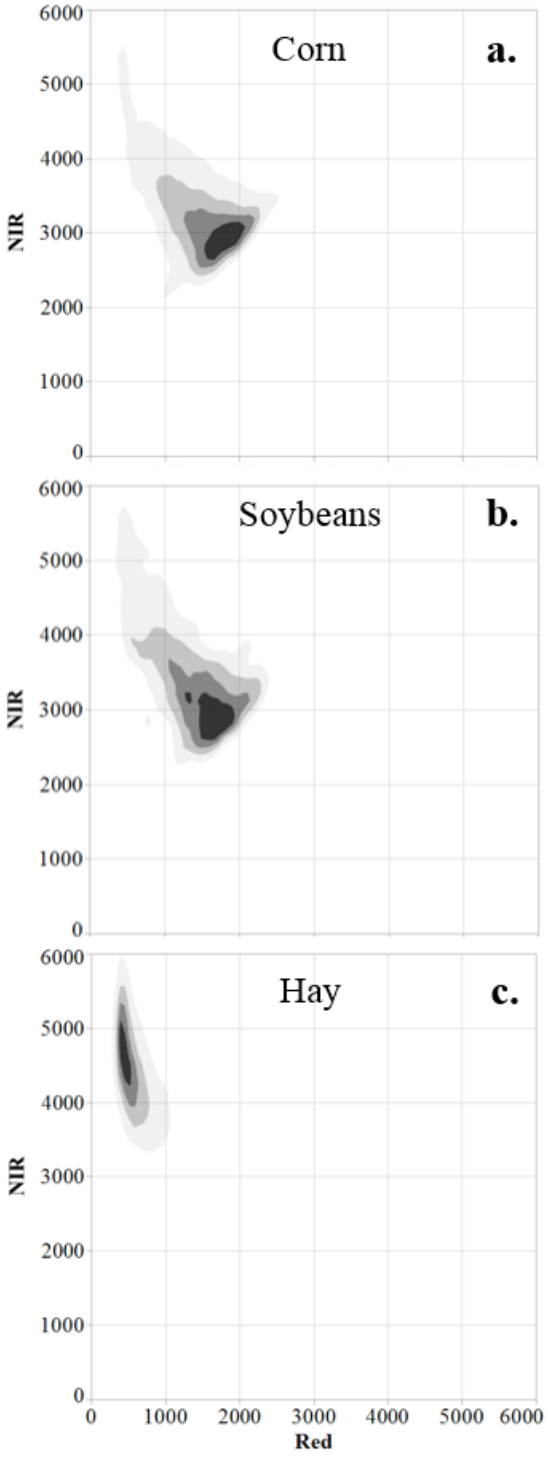

Figure 4.1: Density plots in Red-NIR spectral space, of the main crop types: corn, soybeans and hay.

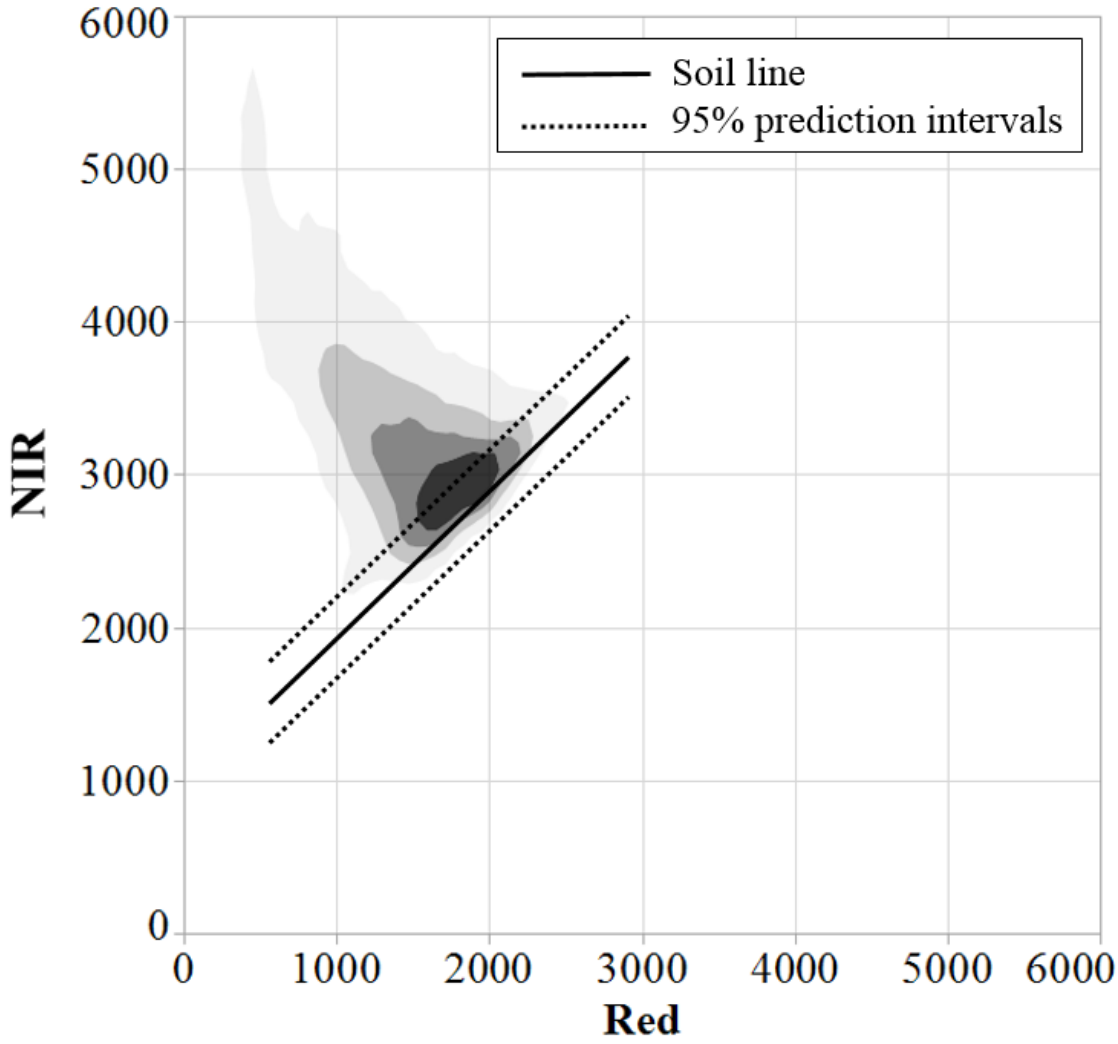

Figure 4.2: Density plot in Red-NIR spectral space of corn and soybeans, with the corresponding soil line (NIR = 958 + 0.9626*Red) and 95% prediction intervals.

4.2 Wetness Calculation

We estimated wetness index values using the soil line method. We calculated the soil line (Figure 4.2), and estimated wetness by calculating the distance along the soil line. To normalize the pixels' calculated distances along the soil line, we first calculated the minimum and maximum distance values. We selected a sub-set of

pixels using the 95 percent prediction intervals representative of bare soil (Figure 4.2). Then, we plotted these pixels' distances along the soil line in a frequency distribution (Figure 4.3) and extracted the 2.5 percent and 97.5 percent quantiles, which we set as the minimum and maximum distance values for the normalization procedure (Table 4.1). We normalized the distances with these statistically derived values and generated wetness index values for all the pixels that ranged between 0 and 1 (Figure 4.4). Wetness index values in the study area varied widely, and averaged 0.422.

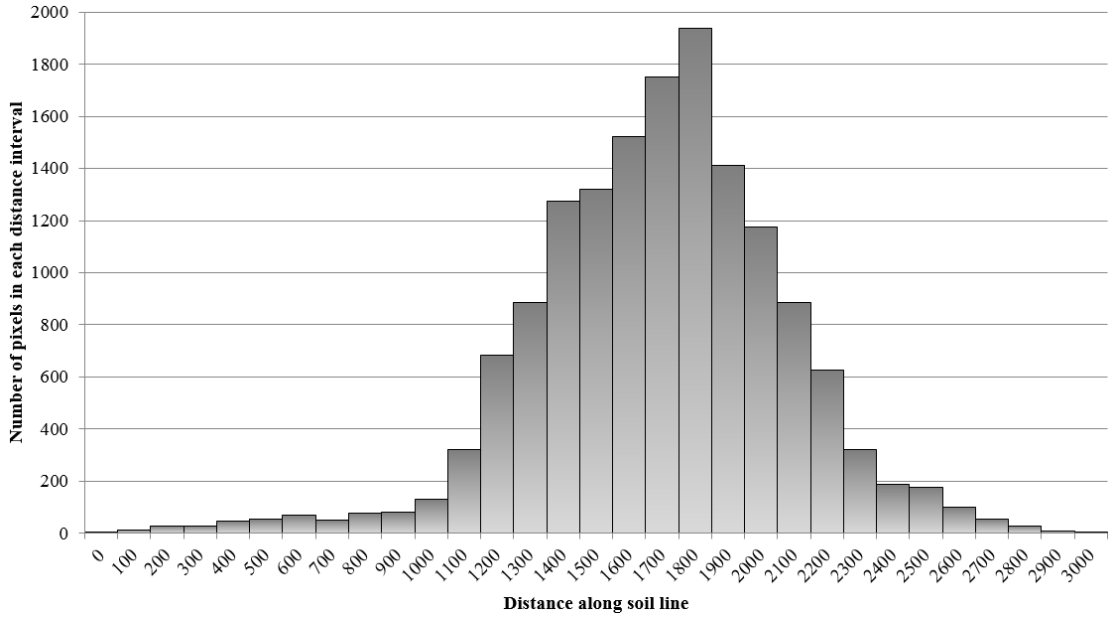

Figure 4.3: Histogram of distance along the soil line of bare soil pixels of corn and soybeans.

Table 4.1: Percentiles of distance values along the soil line. The 97.5 and 2.5 percentiles are used to normalize the distance values.

Percentile (%)	Distance along the soil line
100	2974.37
99	2540.72
97.5	2389.27
95	2231.93
75	1879.53
50	1659.13
25	1405.71
5	1063.15
2.5	821.97
1	465.00
0	0.00

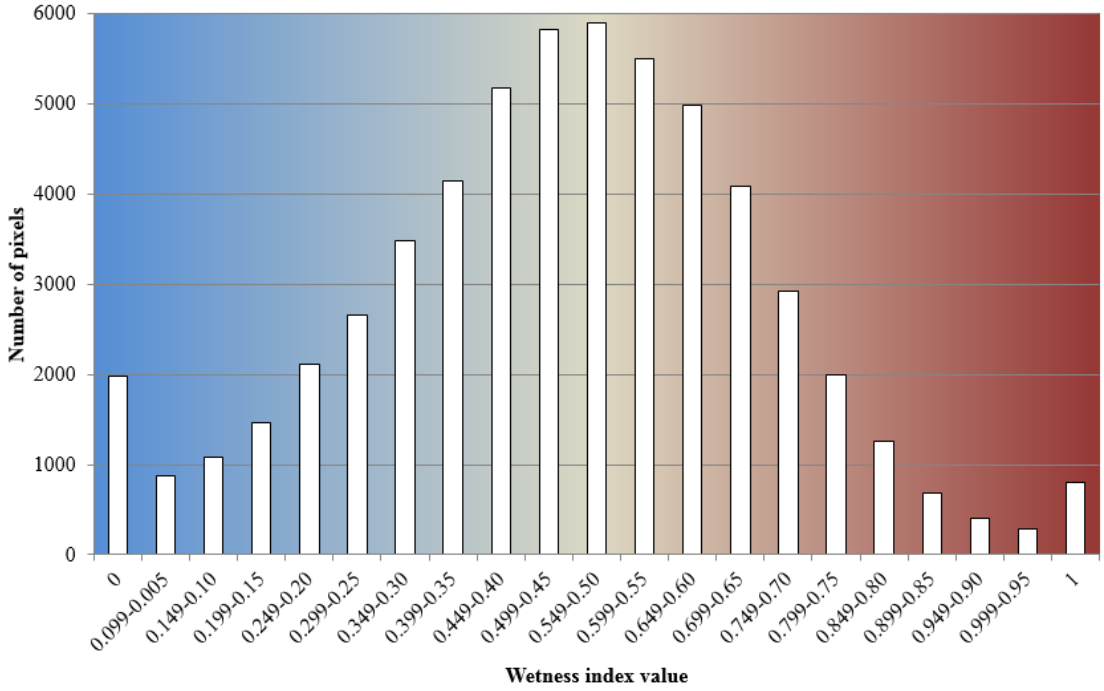

Figure 4.4: Histogram of wetness index values for corn and soybeans pixels.

4.3 Validation

4.3.1 Single-scene spectral validation

The reference sites' locations along the soil line are expected to reflect their respective moisture content. "Compost piles", with high organic matter, should be situated lower on the soil line due to their high moisture content (Figure 4.5). "Fields with compost" would theoretically fall slightly higher on the soil line. "Fields without compost" would fall much higher along the soil line, due to their drier soils (Figure 4.5).

In our analysis, we found the three types of reference sites were mostly situated along their expected regions of the soil line (Figure 4.6). The spectral response of "compost piles" reflected its expected high moisture content. Many sites

representing “fields with compost” illustrated that compost application to farm fields increases the moisture holding capacity of the soil (Figure 4.6). The position of “fields without compost” higher along the soil line indicated that these sites had less organic matter to retain soil moisture. Overall, these results confirmed that the high organic matter and moisture content in mushroom compost could be detected with this remote sensing methodology.

The results also illustrate that most of the agricultural fields in the study area had low to moderate levels of compost. “Fields with compost” and “fields without compost” were situated inside the density cluster where most of the pixels fall along the soil line (Figure 4.6).

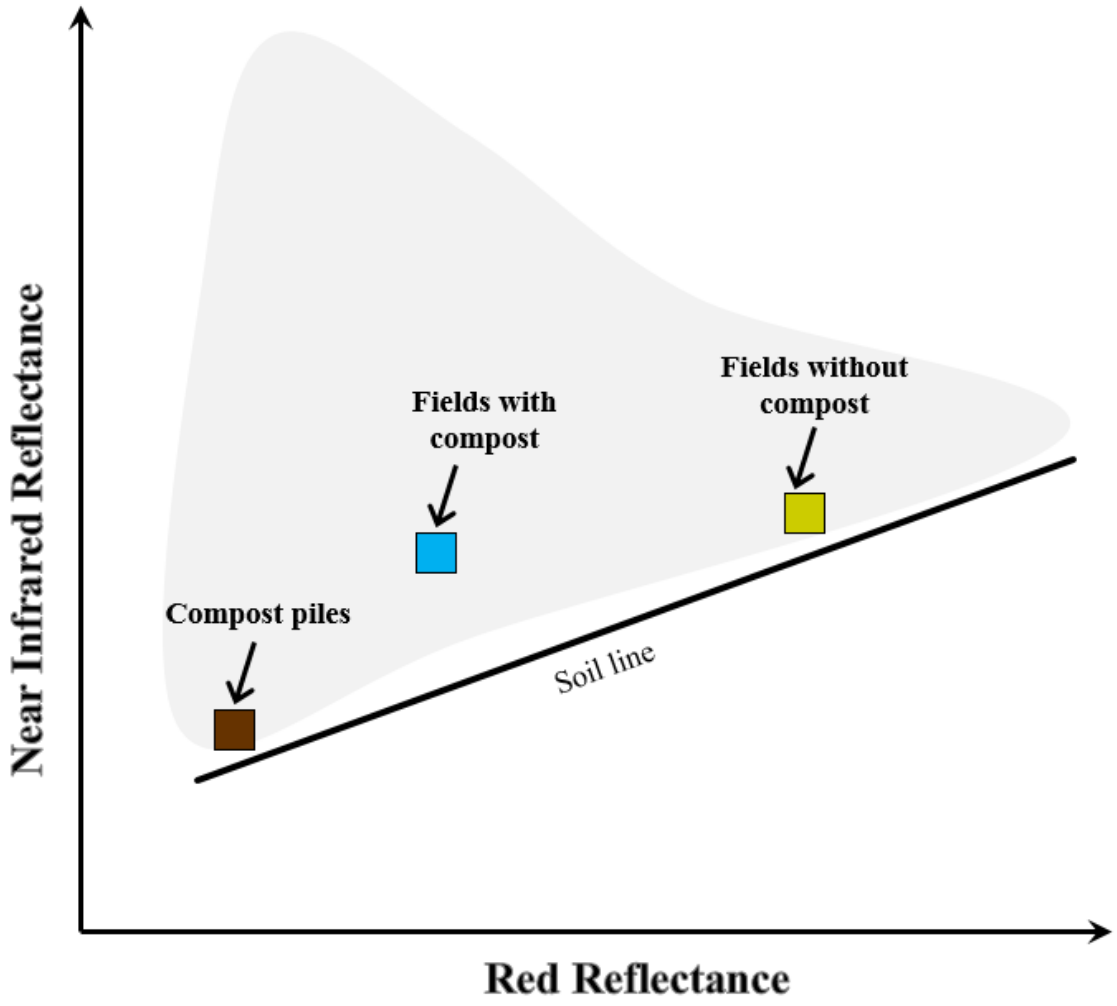

Figure 4.5: Conceptual diagram of the spectral responses of soils with different amounts of mushroom compost.

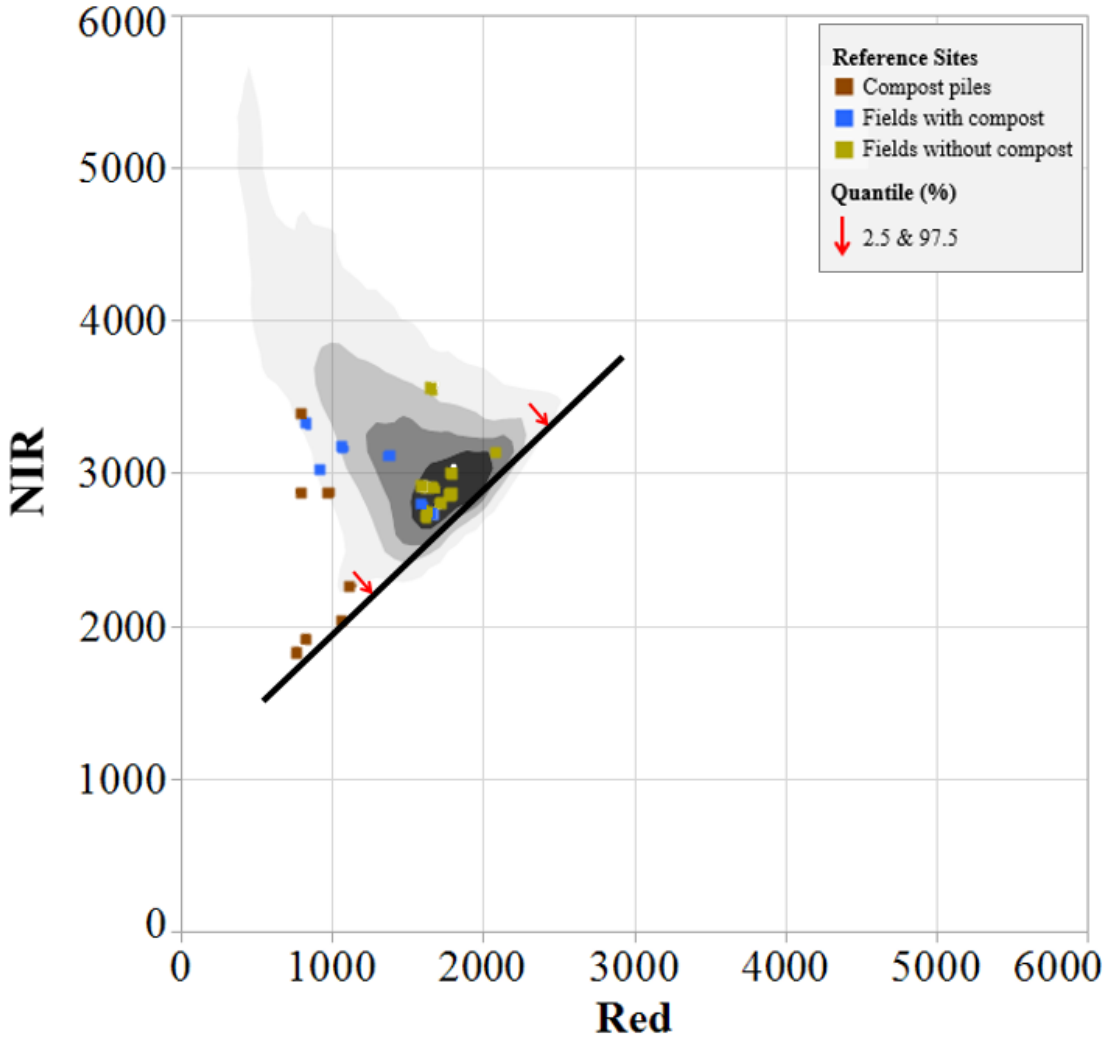

Figure 4.6: Positioning of the compost reference sites along the soil line in Red-NIR spectral space.

4.3.2 Multi-scene temporal spectral validation

The three types of reference sites should produce different temporal patterns over the growing season (Figure 4.7). “Compost piles” would remain lower in spectral space since they contain the highest amount of organic matter and therefore remain moist throughout the year (Figure 4.7). For agricultural fields, the spectral response

should be situated in different portions of spectral space, depending on seasonal changes in crop cover. We expect “fields with compost” to form a narrow temporal pattern that travels a short distance along the soil line because they would retain moisture in fields during the dry spring months. We expect “fields without compost” to form a wide temporal pattern that travels further along the soil line. The wide temporal pattern in “fields without compost” indicates a greater range of moisture in the field throughout the growing season. The greater range of moisture is caused by having relatively less organic matter to retain moisture during the dry 2011 spring months.

Overall, the results from the temporal analysis showed that the reference sites maintained their relative positions in spectral space throughout the growing season. “Compost piles” displayed a tight temporal pattern that was positioned in the lower portion of the Red-NIR spectral plot (Figure 4.8). This suggests that “compost piles” remained moist and were least affected by vegetation effects. “Fields with compost” demonstrated a tighter temporal pattern in spectral space than “fields without compost”. These results validate our methodology to estimate compost application from differences in soil moisture retention.

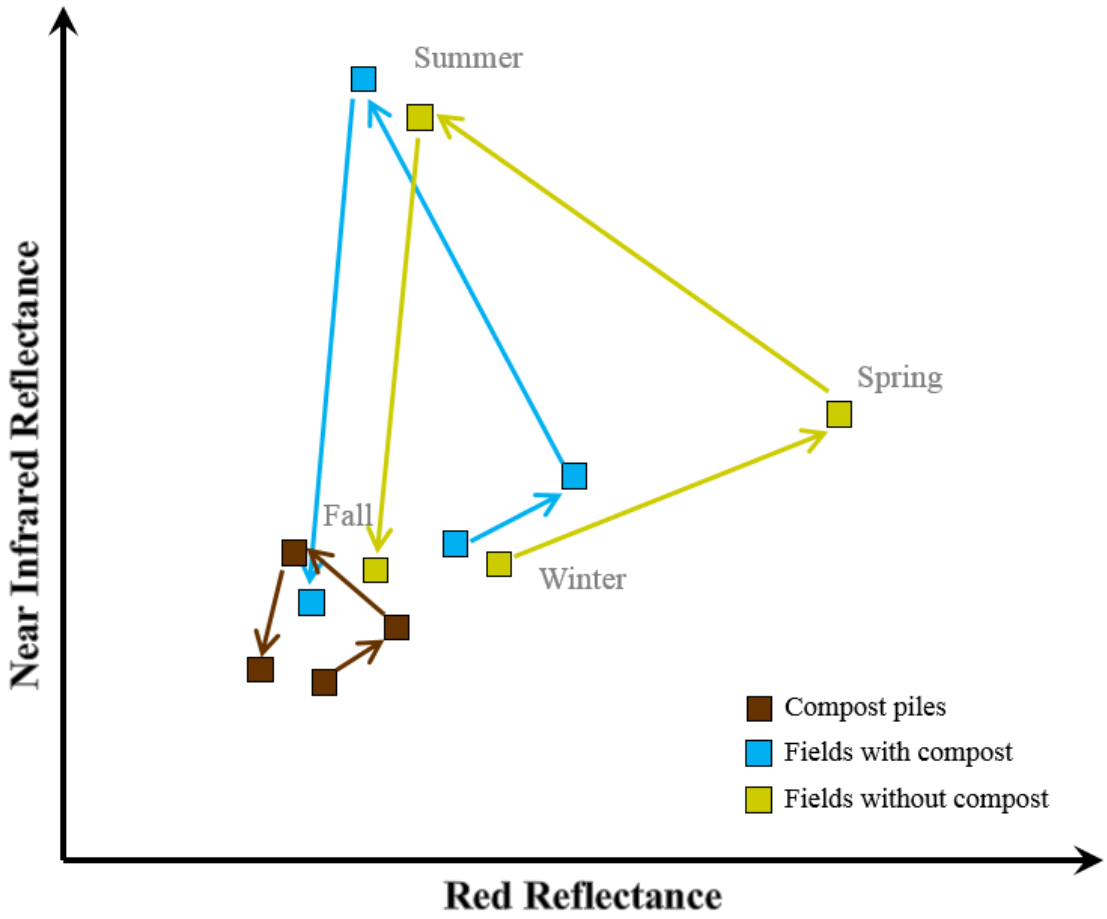

Figure 4.7: Conceptual diagram of the expected temporal patterns in Red-NIR spectral space of the compost reference sites.

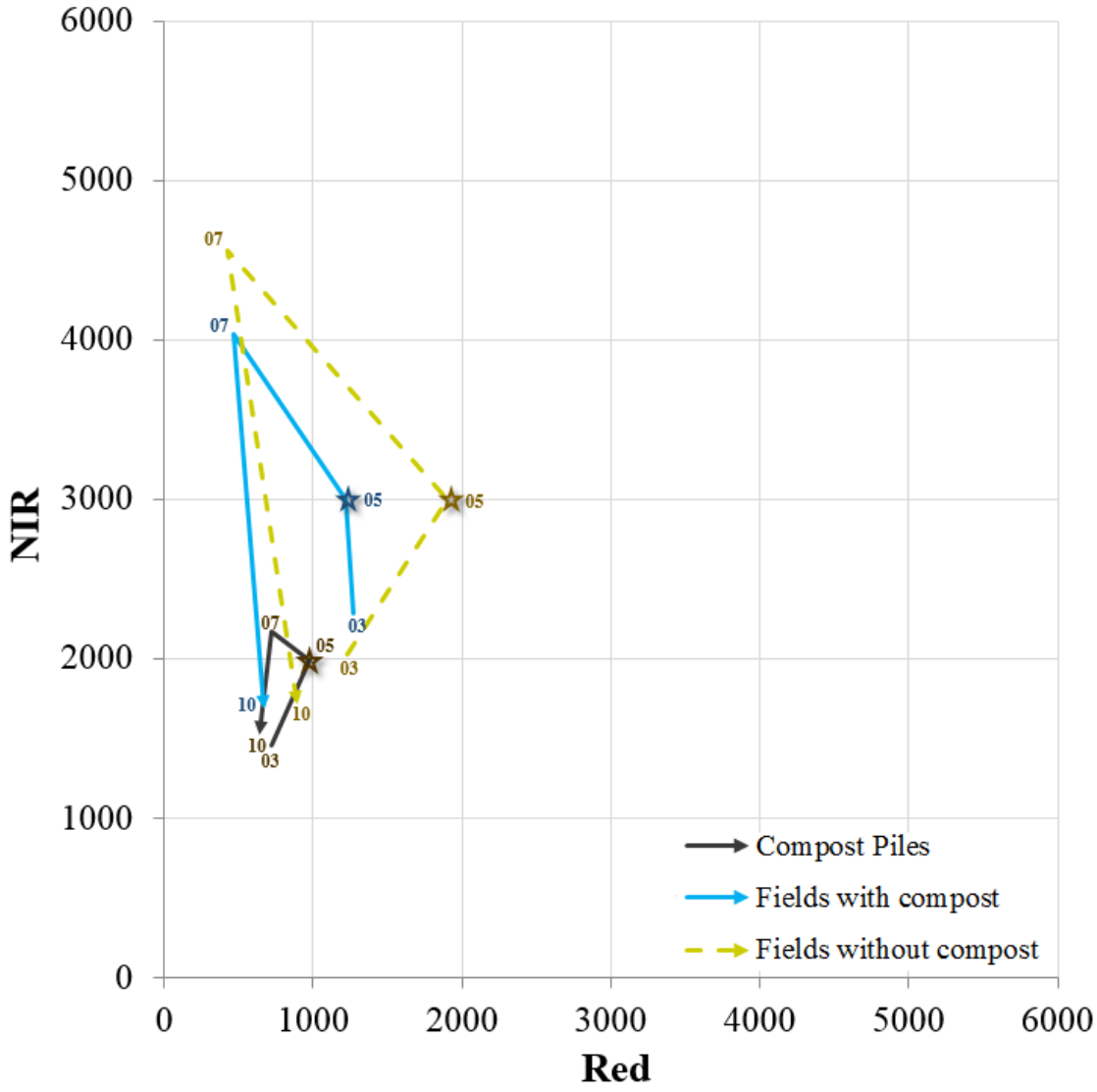

Figure 4.8: Temporal patterns in Red-NIR spectral space of the compost references sites in 2011, for March 08 (03), May 11 (05), July 21 (07), October 25 (10). Star denotes the May 11 scene that was used for calculating wetness index.

4.3.3 Empirical validation using expert knowledge

Results from the expert validation showed that estimated wetness index values were strongly correlated to the empirical compost application rating ($R^2 = 0.96$; $p <$

0.01) (Figure 4.9). Overall, this independent validation analysis proved that our remote sensing methodology produced realistic estimates.

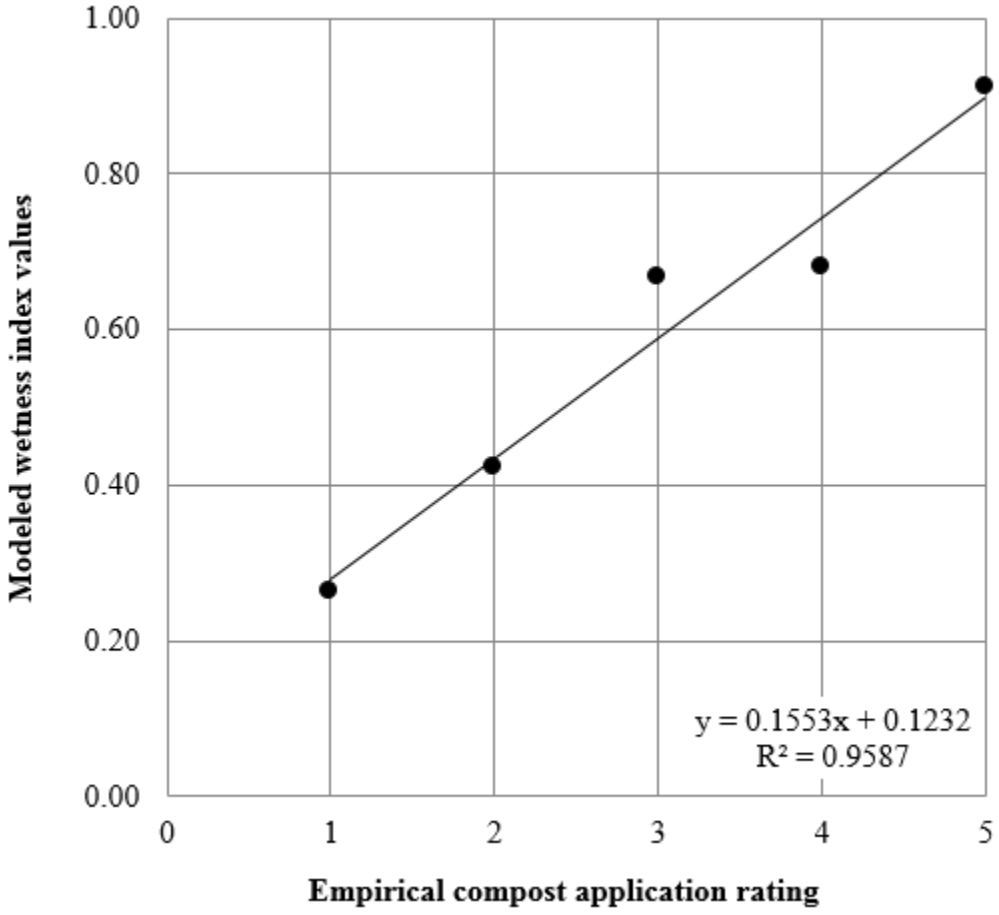

Figure 4.9: Correlation analysis of expert validation, comparing modeled wetness index values (median values) against the empirical compost rating by experts.

4.4 Mapping Wetness

4.4.1 Patterns within passive composting operations

We identified approximately 30 passive composting operations in the study area. To examine the spatial distribution of wetness index within passive composting operations, we selected 18 of the operations for which we calculated soil wetness. These eighteen passive composting operations generally exhibited higher wetness index values than all fields in the study area, demonstrating that compost increases wetness in soils (Figure 4.10; Figure 4.11). The average wetness index value inside these eighteen passive composting operations (0.606) was greater than the average value for all fields in the study area (0.442). Also, there are more wetness index values equal to 1 in farm parcels managing compost (9 percent of wetness index values), than all wetness index values in the study area (1 percent of wetness index values) (Figure 4.4; Figure 4.12). The greater proportion of high wetness index values in farm parcels managing compost suggests that applying compost changes the moisture content in soils. Therefore, high wetness index values in other portions of the study area suggest that these fields were most likely intensely applied with compost.

It is important to understand the fine-scale spatial variation of wetness index values inside passive composting operations to comprehend overall watershed-scale wetness patterns. These wetness index values inside passive composting operations varied between 0 and 1 (Figure 4.12; Figure 4.13). We found low wetness index values inside farms were similar to the spectral response of "fields without compost". For example, low wetness index values in Parcel ID 64 represented a grassy filter area (Figure 4.13; Figure 4.14). Next, moderately-high wetness index values represented crop fields amended with compost, which suggested that compost slightly elevated the

moisture content similar to the spectral response of "fields with compost" (Figure 4.13; Figure 4.14). Of the eighteen composting operations, we selected a subset of 12 operations that have specific areas with large piles of weathering compost. Each of the 12 operations had a very high average wetness index value between 0.76 and 0.97 (Figure 4.15). Also, the spectral signature of these areas with piles of weathering compost was similar to the validation reference sites of "compost piles".

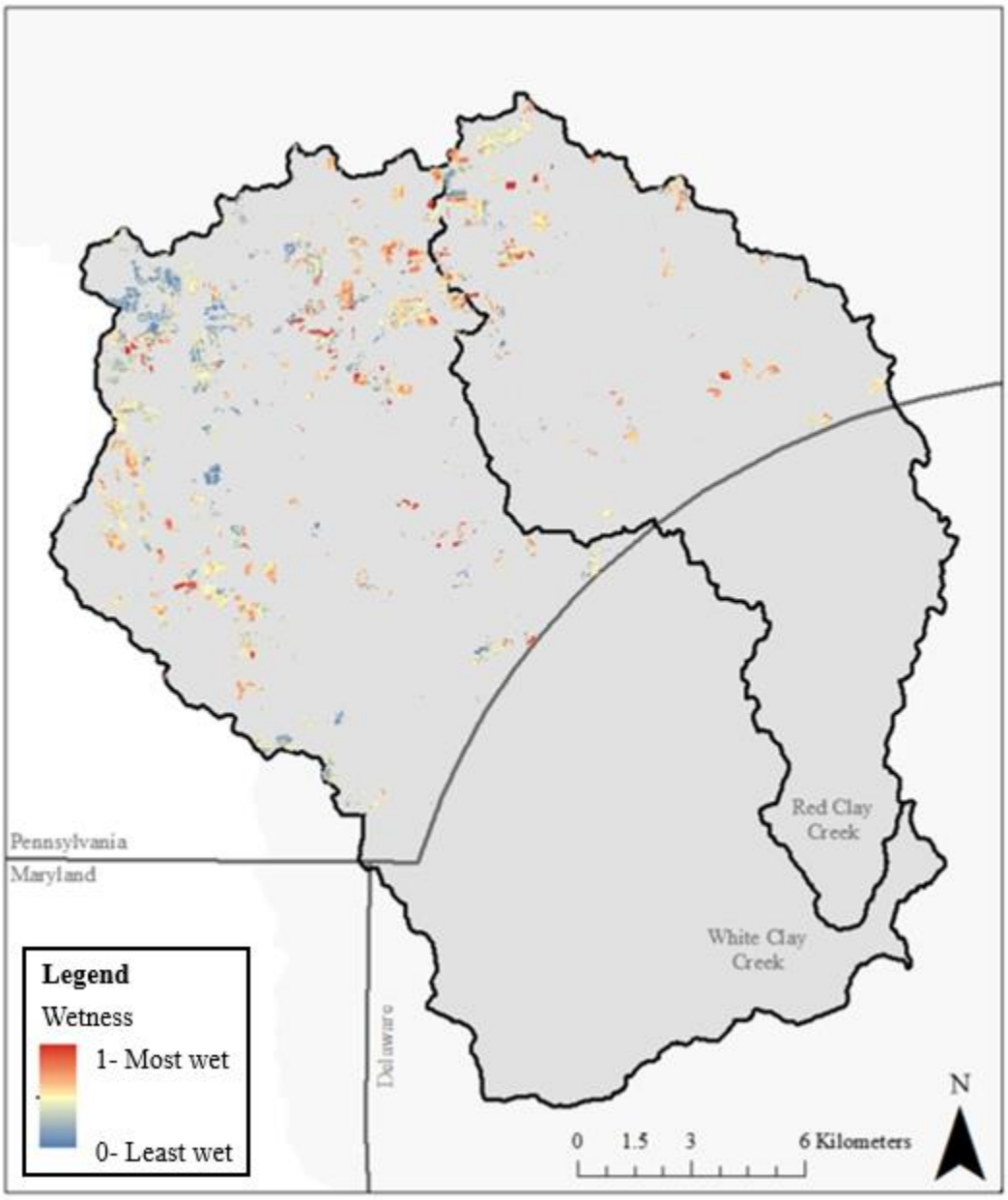

Figure 4.10: Wetness index values of all fields in study area.

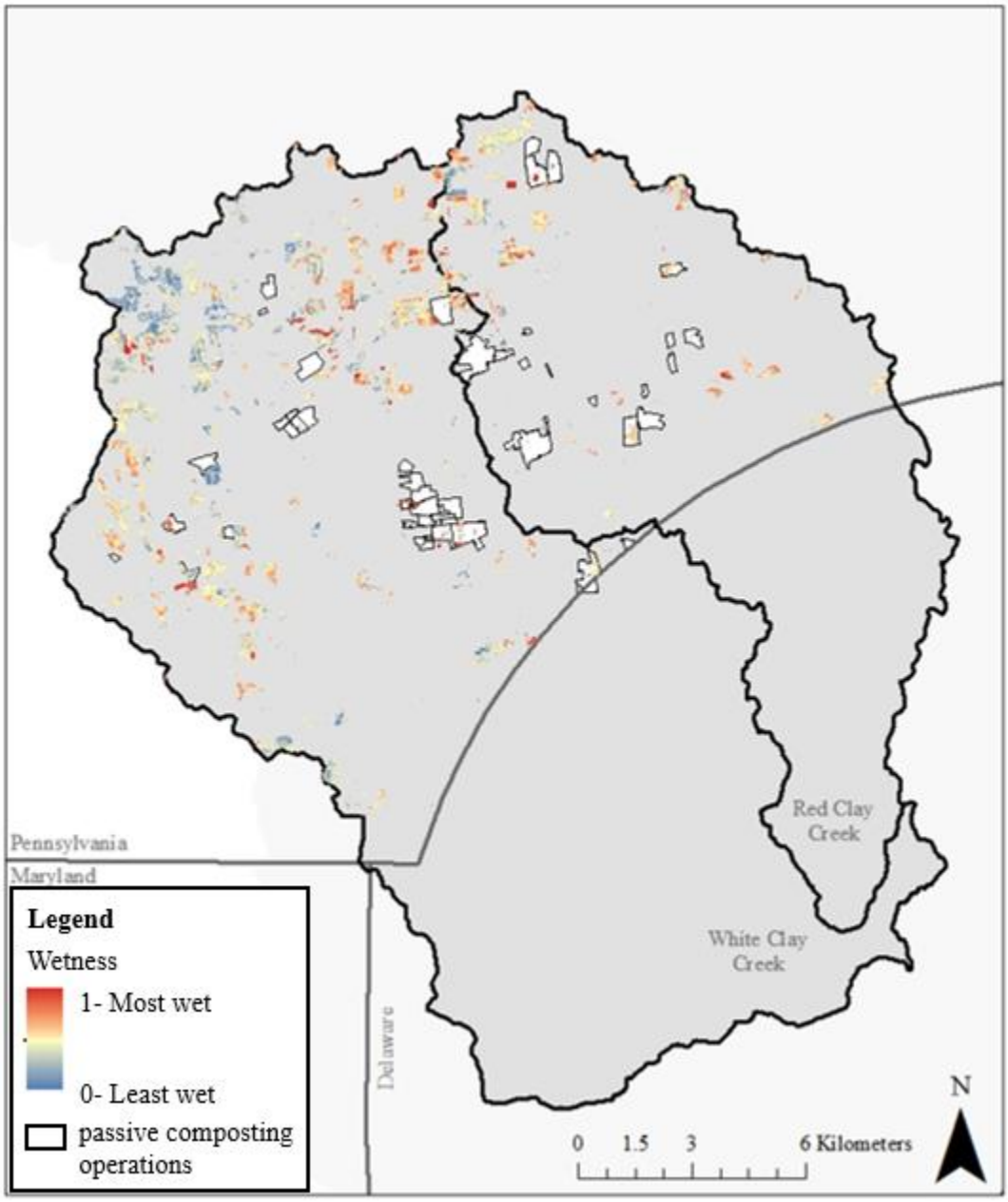

Figure 4.11: Wetness index values and all known passive composting operations in the study area.

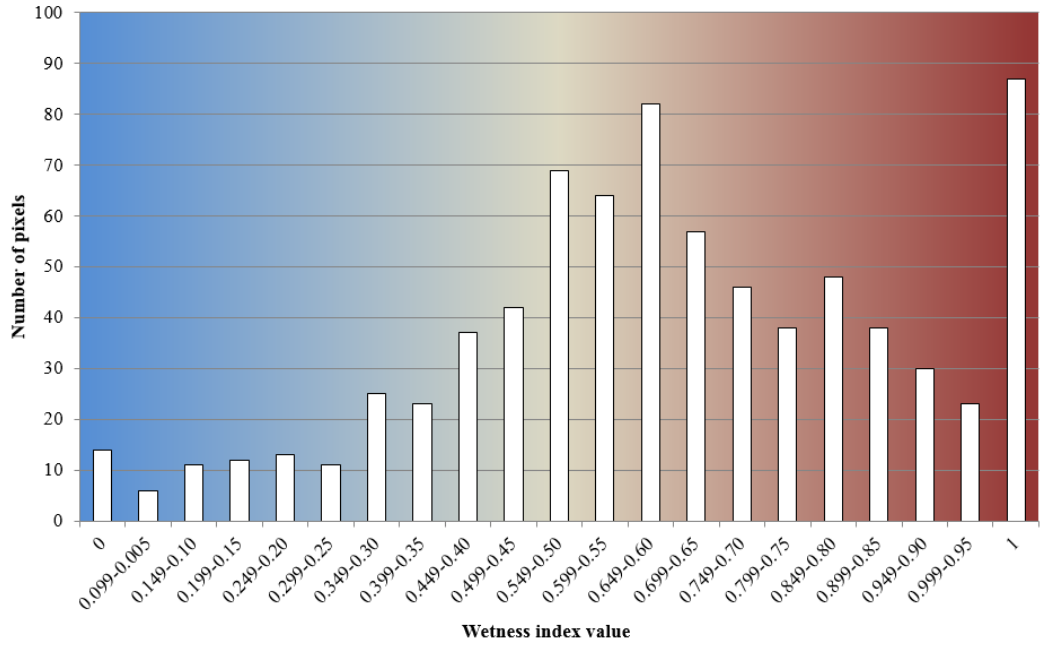

Figure 4.12: Histogram of all wetness index values for the 18 passive composting operations.

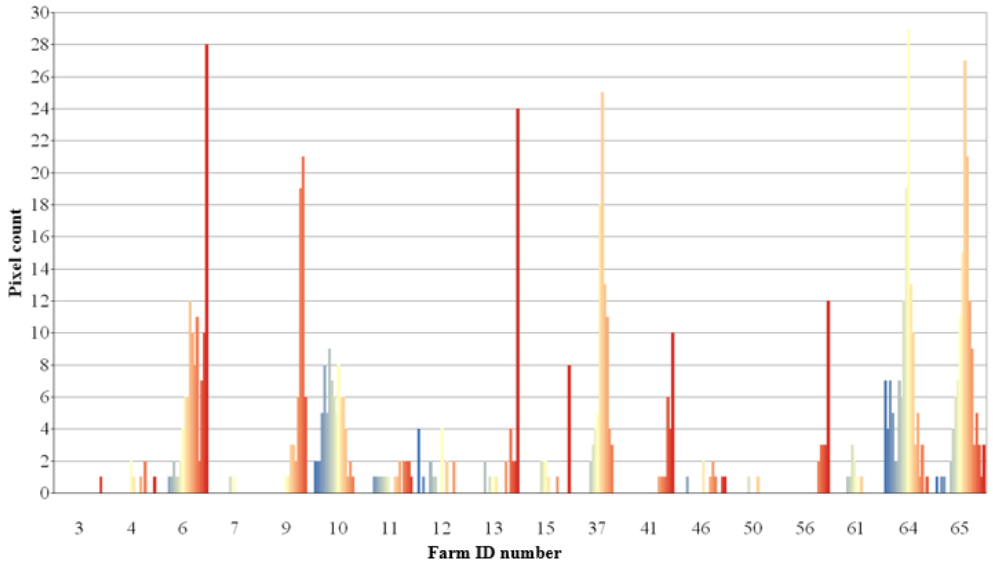

Figure 4.13: Histograms of wetness index values within the 18 individual passive composting operations. Red bars indicate areas in an operation with high wetness index values, suggesting intense compost application. Blue bars indicate areas in an operation with low wetness index values, suggesting little to no compost.

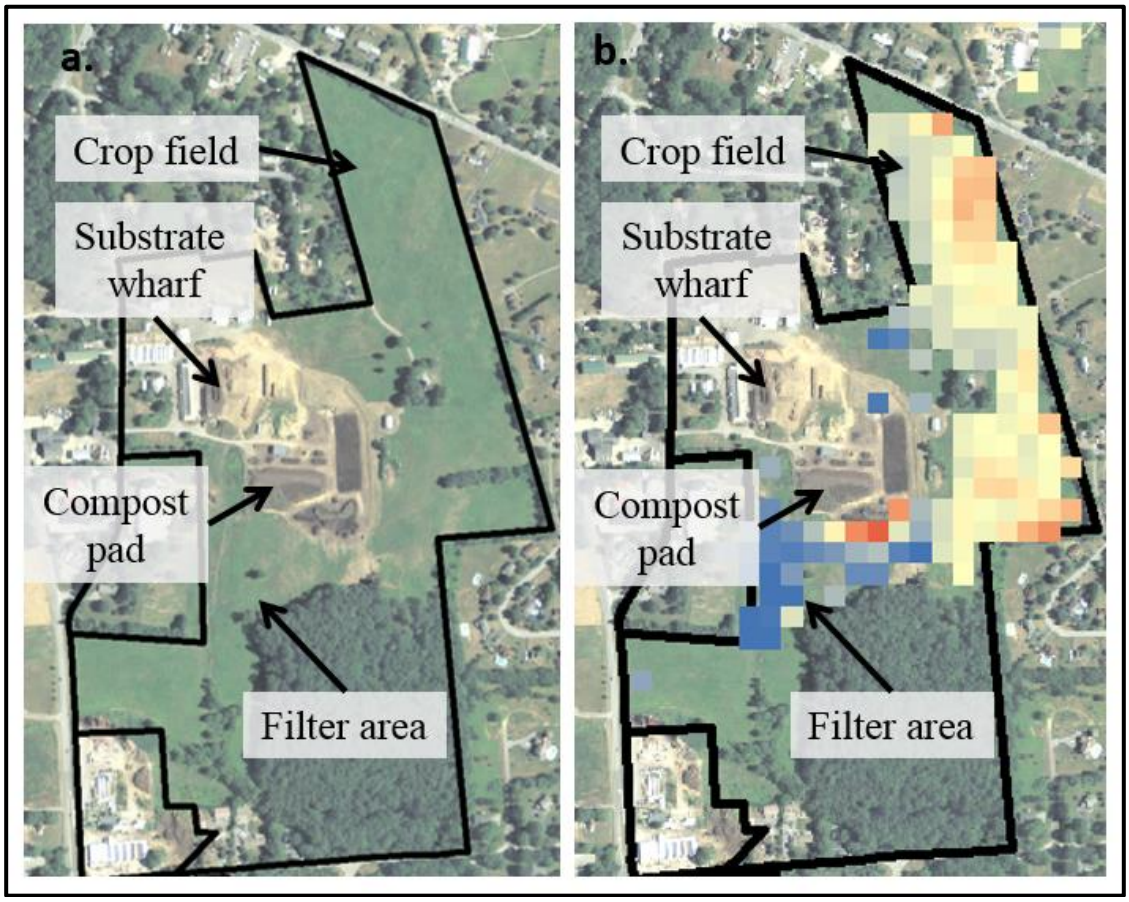

Figure 4.14: Example of an individual passive composting operation (Farm ID 64), showing: (a) land cover; and (b) wetness index values. Note that wetness values are only calculated for fields under corn or soybeans.

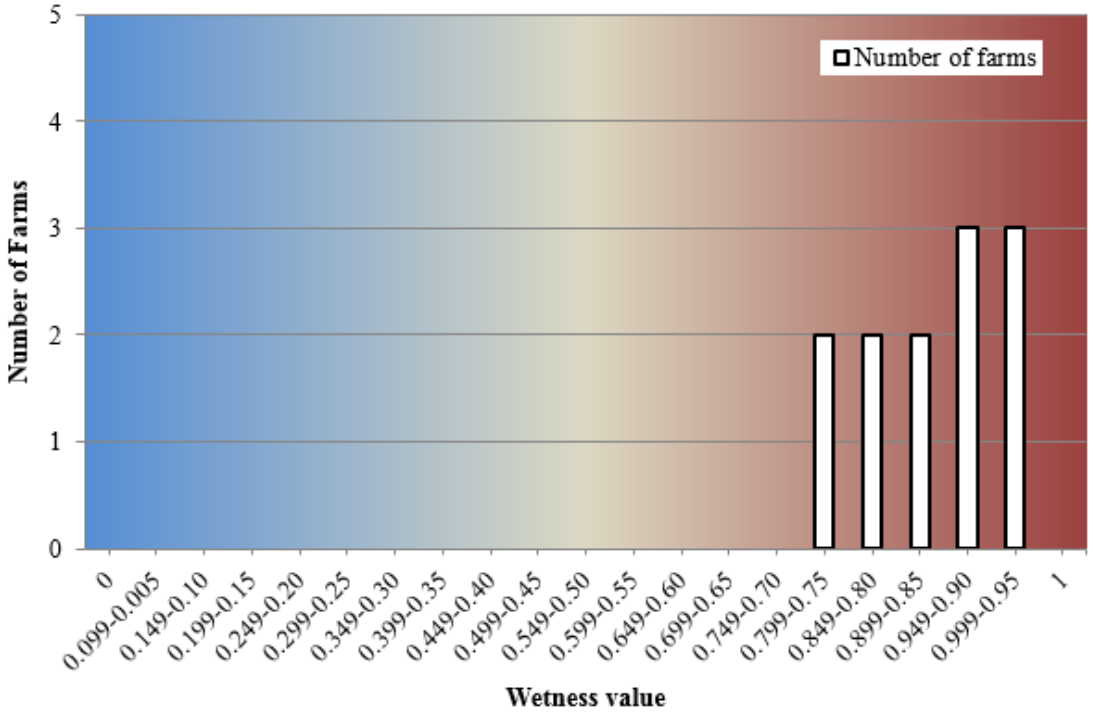

Figure 4.15: Histogram of average wetness index values for a subset of 12 passive composting operations that have specific areas with large piles of weathering compost.

4.4.2 Patterns surrounding passive composting operations

Fields surrounding passive composting operations had overall higher wetness index values. We assume compost was intensely applied to these fields because of their proximity to operations passively weathering spent compost (Tobler's First Law of Geography). Figure 4.16 shows an example of where we used historical imagery from 2010 to confirm field-application of compost near a known passive composting operation. In fact, these nearby fields are leased to passive composting operations for

field application to provide fertilizer and improve soil health (M. Zuk, personal communication, 2016).

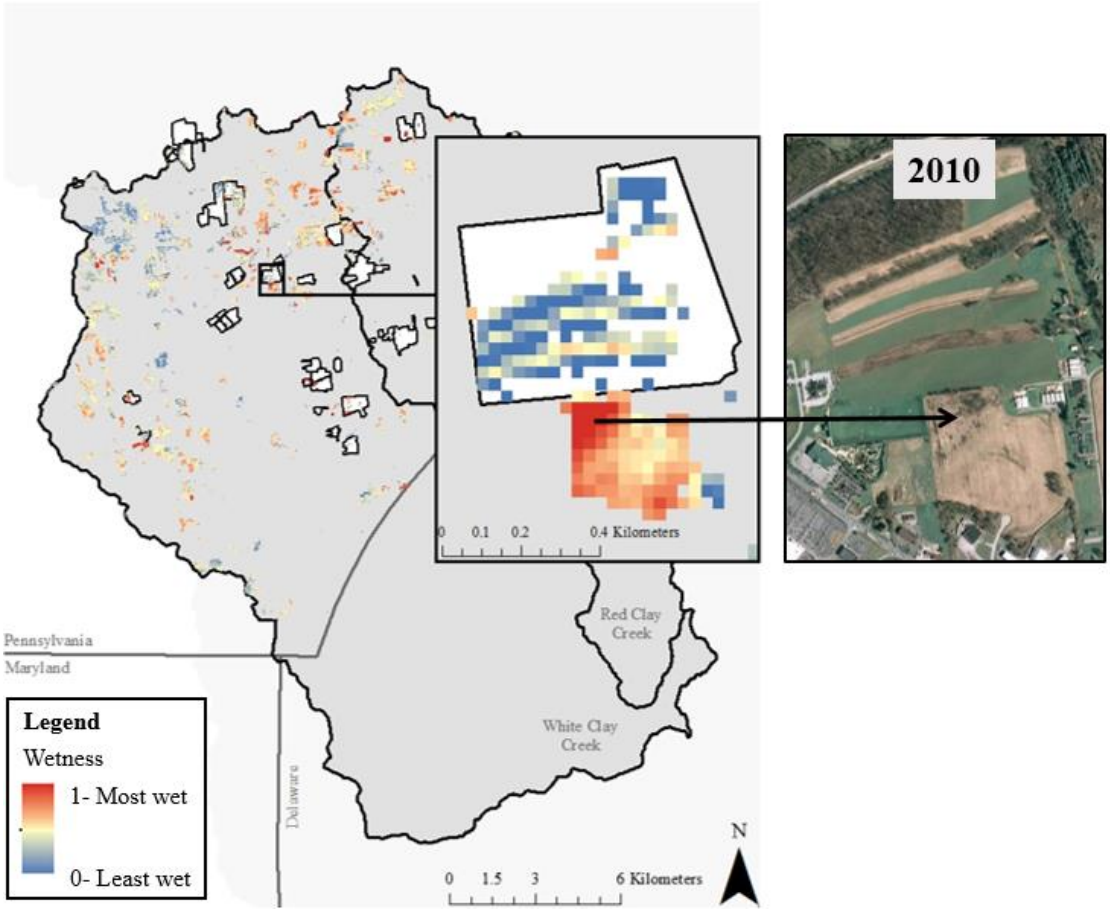

Figure 4.16: Evidence of high-intensity compost application near a passive composting operation. 2010 image courtesy of ChescoViews.

4.4.3 Patterns between crop fields

We observed discrete spatial variation of wetness index values between different crop fields, which suggests that some fields received higher compost application intensities than others. Figure 4.17 illustrates two adjacent crop fields with

contrasting wetness index values. Field A has very high wetness index values, which suggests high intensity compost application. The presence of high compost application rates was also confirmed by local agricultural extension agents during the empirical validation process. In contrast, Field B has low wetness index values, which suggests a much lower rate of compost application; this observation was also confirmed during empirical validation. These spatial patterns of contrasting wetness index values illustrate that our methodology captures discrete variation of compost application rates between different crop fields, and further validates our spatial estimates.

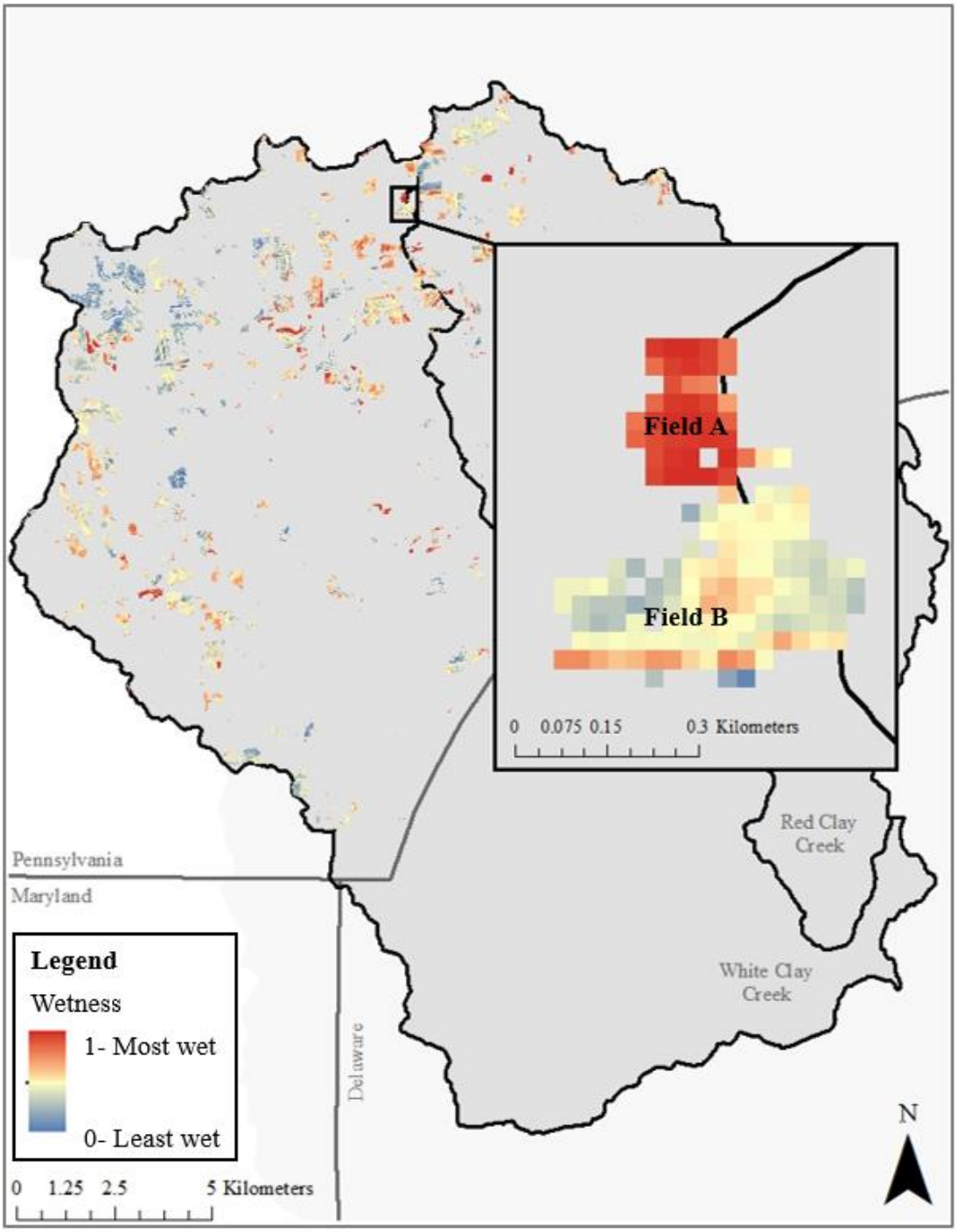

Figure 4.17: Two fields with differences in wetness, demonstrating varying compost application intensities. Field A was intensely applied with compost (M. Zuk, personal communication, 2016). Field B suggests lower compost application intensities.

4.4.4 Patterns across the watersheds

Soil wetness patterns varied across the study area (Figure 4.10). In the northern-most central region of the study area, there were many fields that had higher wetness index values, suggesting fields in this region were intensely applied with compost. It was confirmed by local agricultural extension agents that many fields in these northern regions of the watersheds are leased for compost application. In contrast, the north-western portion of the study area consisted of many fields with low wetness index values. This localized pattern suggests that many fields in this region did not receive compost, or had very low compost application rates that did not affect their soil's moisture retention properties. These fields are part of large-scale animal farming operations, which almost exclusively fertilize their crop fields with manure. These key spatial patterns of compost application, and their intensities, were confirmed by experts from the local agricultural extension.

We also observed patterns of relatively high wetness in the western-most region of the study area (Figure 4.10). During the validation of field-scale wetness estimates, experts were unsure of the extent or intensity of compost application in several fields that were situated within this portion of the study area.

Wetness patterns across the central region of the study area mainly consisted of small fields with very high wetness index values, suggesting localized areas of intense compost application (Figure 4.10). These fields are generally located near substrate production facilities, mushroom growing facilities, and passive composting operations.

4.5 Factors Influencing Wetness

Besides compost, other factors can increase or decrease a wetness index value which can potentially interfere with the accuracy in our estimates of a field's compost

application intensity. These factors include fresh manure application, and the spatial resolution of the image. We speculate that fresh manure application before scene acquisition can increase a field's overall wetness index value. When manure is freshly applied to fields, there is initial moisture and darkening of the soil which can cause a decrease in spectral reflectance, and therefore depicts high wetness. During expert validation, we found some sample sites that were applied with manure had high wetness values. These few sites were considered outliers, because most of the other sites that had manure application (and no compost) had low wetness index values. It is therefore possible that these particular fields with high wetness values were influenced by the fresh application of manure.

Also the coarse spatial resolution of the Landsat imagery could affect the accuracy. Even though the imagery produces realistic general patterns of wetness at coarse scales, at the individual 30m pixel scale the values of wetness index are sometimes distorted, especially along field boundaries. This distortion is because of spectral mixing, when an individual pixel contains more than one land-use type (Jenson, 2007).

Chapter 5

CONCLUSIONS AND RECOMMENDATIONS

5.1 Conclusions

The goal of this study was to estimate the spatial extent and intensity of field-applied mushroom compost. We applied a remote sensing approach using Landsat multispectral imagery, and used the soil line technique to detect differences in soil wetness as a result of compost application. This is the first study that uses remote sensing to map field-applied compost from the field-scale to the watershed scale. From this research we conclude that:

1. The soil line based wetness index worked well for estimating spatial distributions of field-applied mushroom compost. We used Landsat imagery, which has a fairly coarse resolution. Through careful scene selection we were able to detect large spatial variation in soil wetness from varying rates of compost application. In this study we used a scene early in the 2011 growing season, when fields were relatively unaffected by vegetation (bare soil conditions) and when antecedent moisture conditions were low.

2. The spectral validation clearly illustrated that compost changes the spectral response of soil because of changes in wetness. The three types of compost application intensities fell within their respective region of the soil line.

3. The independent expert validation of field-scale wetness produced a strong significant correlation between our remotely-sensed wetness estimates and the empirical ratings of compost application intensities provided by experts.

4. The methodology produced realistic spatial distributions of field-applied mushroom compost application intensities across the study area and across multiple spatial scales, from the field-scale to the watershed scale.

5.2 Recommendations

We recommend using the results from this study to aid watershed restoration efforts. The spatial distributions of compost application intensity are currently used by Luc Claessens et al. in follow-up studies to assess the effect of spent mushroom compost on stream water quality in the Brandywine-Christina River Basin. The methodology used in this study can also be easily transferred to other geographical areas that manage spent mushroom compost and similar organic fertilizers.

For future research, we recommend using higher spatial resolution imagery to have less distortion from spectral mixing and obtain a more accurate estimate of discrete spatial variation of compost application intensities. We also recommend updating this map every 10 years, or more frequently, depending on available remote sensing imagery and optimal crop growth and soil moisture conditions.

REFERENCES

Anderson, K., and H. Croft (2009), Remote sensing of soil surface properties, Prog. Phys. Geogr., 33(4), 457–473, doi:10.1177/0309133309346644.

BAE Systems (2007), Chester County, Pennsylvania land use/ land cover dataset 2005, using Esri ArcGIS 10.1.1.3143

Baret, F., S. Jacquemoud, and J. F. Hanocq (1993), The soil line concept in remote sensing, Remote Sens. Rev., 7(1), 65–82, doi:10.1080/02757259309532166.

Ben-Dor, E. (2002), Quantitative remote sensing of soil properties, Adv. Agron., 75, 173–243

Beyer, D. M. (2003), Basic procedures for Agaricus mushroom growing, 16 pp., Pennsylvania State University, University Park, Pennsylvania.

Buja, K., and C. Menza (2013), Sampling Design Tool for ArcGIS, National Oceanic and Atmospheric Administration Biogeography Branch

Caloz, R., B. Abednego, and C. Collet (1988), The normalization of a soil brightness index for the study of changes in soil conditions, Proc. 4th Int. Colloq. Spectr. signatures objects Remote Sens., (MARCH 1988), 18–22.

Charles, D. (2012), How a sleepy Pennsylvania town grew into America's mushroom capital, *Natl. Public Radio*, 11th October.

Chester County Agricultural Development Council (2012), *Agricultural info sheet: field crops in Chester County*, Chester County, Pennsylvania.

Chester County Agricultural Development Council (2012), *Agricultural info sheet: Chester County census of agriculture*, Chester County, Pennsylvania.

Chester County Agricultural Development Council (2012), *Agricultural info sheet: mushrooms in Chester County*, Chester County, Pennsylvania.

Chester County DCIS/GIS (2011), Chester County Municipal Boundaries, http://www.pasda.psu.edu, West Chester, Pennsylvania.

Chester County Pennsylvania Land Record System (GIS) (n.d.), ChescoViews R3.1, Available from: https://arcweb.chesco.org/cv3/

Chester County Water Resources Authority, Chester County Planning Commission, Camp Dresser and McKee, G. P. L. (2002), Red Clay Creek: Watershed action plan, 1-85, Chester County, Pennsylvania.

Croft, H., N. J. Kuhn, and K. Anderson (2012), On the use of remote sensing techniques for monitoring spatio-temporal soil organic carbon dynamics in agricultural systems, Catena, 94, 64–74, doi:10.1016/j.catena.2012.01.001.

Cruz-Ortiz, C., and K. Miller (2014), The economic value of the Christina Basin, 10 pp., University of Delaware Water Resources Agency, Newark, Delaware.

Delaware Environmental Observing System (DEOS) (n.d.), Daily precipitation and soil moisture data (2009-2014), Available from: http://www.deos.udel.edu/ (Accessed 12 May 2015)

Delaware Office of State Planning Coordination (2013), Municipalities, http://opendata.firstmap.delaware.gov/, Dover, Delaware

Dellinger, A. E., J. P. Schmidt, and D. B. Beegle (2008), Developing nitrogen fertilizer recommendations for corn using an active sensor, Agron. J., 100(6), 1546, doi:10.2134/agronj2007.0386.

Demattê, J. A. M., A. A. Sousa, M. C. Alves, M. R. Nanni, P. R. Fiorio, and R. C. Campos (2006), Determining soil water status and other soil characteristics by spectral proximal sensing, Geoderma, 135, 179–195, doi:10.1016/j.geoderma.2005.12.002.

Dupigny-Giroux, L.-A., and J. E. Lewis (1999), A moisture index for surface characterization over a semiarid area, Photogramm. Eng. Remote Sens., 65(8), 937–945.

ESRI (2014), Available water storage 0-150 cm - weighted average map package, Soil Survey Staff, US Natural Resources Conservation Service, US Department of Agriculture. Soil Survey Geographic (SSURGO) Database. Available online at http://soildatamart.nrcs.usda.gov

ESRI (2016), ArcGIS 10.1st ed.

Fidanza, M. a., D. L. Sanford, D. M. Beyer, and D. J. Aurentz (2010), Analysis of fresh mushroom compost, Hort technology, 20(2), 449–453.

Flammini, S. (1999), The evolution of the mushroom industry in Kennett Square, Available from: http://courses.wcupa.edu/jones/his480/reports/mushroom.htm (Accessed 8 April 2016)

Fox, G. a., and G. J. Sabbagh (2002), Estimation of soil organic matter from red and near-infrared remotely sensed data using a soil line euclidean distance technique, Soil Sci. Soc. Am. J., 66(6), 1922, doi:10.2136/sssaj2002.1922.

Fox, G. a., G. J. Sabbagh, S. W. Searcy, and C. Yang (2004), An automated soil line identification routine for remotely sensed images, Soil Sci. Soc. Am. J., 68(4), 1326, doi:10.2136/sssaj2004.1326.

Frazier, B. E., and Y. Cheng (1989), Remote sensing of soils in the eastern Palouse region with Landsat Thematic Mapper, Remote Sens. Environ., 28(August 1988), 317–325, doi:10.1016/0034-4257(89)90123-5.

Gao, Z., X. Xu, J. Wang, H. Yang, W. Huang, and H. Feng (2013), A method of estimating soil moisture based on the linear decomposition of mixture pixels, Math. Computer. Modeling, 58(3-4), 606–613, doi:10.1016/j.mcm.2011.10.054.

Ghulam, A., Q. Qin, and Z. Zhan (2007), Designing of the perpendicular drought index, Environ. Geol., 52(6), 1045–1052, doi:10.1007/s00254-006-0544-2.

Guo, M., J. Chorover, and R. H. Fox (2001a), Effects of spent mushroom substrate weathering on the chemistry of underlying soils, J. Environ. Qual., 30(6), 2127–2134, doi:10.2134/jeq2001.2127.

Guo, M., J. Chorover, R. Rosario, and R. H. Fox (2001b), Leachate chemistry of field-weathered spent mushroom substrate, J. Environ. Qual., 30(5), 1699–1709, doi:10.2134/jeq2001.3051699x.

Guo, M., and J. Chorover (2004), Solute Release from Weathering of Spent Mushroom Substrate under Controlled Conditions, Science., 12(3), 225–234, doi:10.1080/1065657X.2004.10702187.

Huete, a. R., G. Hua, J. Qi, A. Chehbouni, and W. J. D. Van Leeuwen (1992), Normalization of multidirectional red and NIR reflectances with the SAVI, Remote Sens. Environ., 41(1992), 143–154, doi:10.1016/0034-4257(92)90074-T.

Jackson, R. D. (1983), Spectral indices in N-Space, Remote Sens. Environ., 13(5), 409–421, doi:10.1016/0034-4257(83)90010-X.

Jensen, J. R. (2007), *Remote sensing of the environment: an earth resource perspective*, 2nd ed., edited by J. Howard, Pearson Prentice Hall, Upper Saddle River.

Kaplan, L. A. (1995), Impact on water quality of high and low density applications of spent mushroom substrate to agricultural lands, Compost Sci. Util., 3(1), 55–63.

Kauth, R. J., and G. S. Thomas (1976), The tasseled cap - A graphic description of the spectral-temporal development of agricultural crops as seen by Landsat, presented at the Symposium on Machine Processing of Remotely Sensed Data, West Lafayette, Indiana, U.S.A

Ladoni, M., H. A. Bahrami, S. K. Alavipanah, and A. A. Norouzi (2010a), Estimating soil organic carbon from soil reflectance: a review, Precis. Agric., 11(1), 82–99, doi:10.1007/s11119-009-9123-3.

Ladoni, M., S. K. Alavipanah, H. A. Bahrami, and A. A. Noroozi (2010b), Remote sensing of soil organic carbon in semi-arid region of Iran, Arid L. Res. Manag., 24(4), 271–281, doi:10.1080/15324982.2010.502917.

Landschoot, P., and A. McNitt (n.d.), Using spent mushroom substrate (mushroom soil) as a soil amendment to improve turf, *Pennsylvania State Univ.* Available from: http://plantscience.psu.edu/research/centers/turf/extension/factsheets/mushroom-soil (Accessed 14 June 2016)

Lou, Z., J. Zhu, Z. Wang, S. A. Baig, L. Fang, B. Hu, and X. Xu (2015), Release characteristics and control of nitrogen, phosphate, organic matter from spent mushroom compost amended soil in a column experiment, Process Saf. Environ. Prot., 98, 417–423, doi:10.1016/j.psep.2015.10.003.

McKay, G. (2008), A fungus humongous: Pennsylvania is No. 1 in growing mushrooms, *Pittsburgh Post-Gazette*, 28th August, Pittsburgh, Pennsylvania.

Miller, K. (2014), A comparative analysis of source water protection policies and regulations of local governments in the Christina River Basin in Delaware and Pennsylvania, M.S. thesis, 167 pp., Water Science and Policy, University of Delaware, Newark, Delaware.

Mulla, D. J. (2013), Twenty five years of remote sensing in precision agriculture: Key advances and remaining knowledge gaps, Biosyst. Eng., 114(4), 358–371, doi:10.1016/j.biosystemseng.2012.08.009.

Muller, E., and H. Dècamps (2000), Modeling soil moisture reflectance, Remote Sens. Environ., 76(2), 173–180, doi:10.1016/S0034-4257(00)00198-X.

Narvaez, M., and A. Homsey (2016), *White Clay Creek state of the watershed report*, 48 pp., University of Delaware Water Resources Agency, Newark, Delaware.

Pennsylvania Department of Environmental Protection (PADEP) (2012), Best Practices for Environmental Protection in the Mushroom Farm Community, 254-5401-001, 57 pp., Harrisburg, Pennsylvania

Pennsylvania Department of Environmental Protection (2003), Watershed Restoration Action Strategy (WRAS) state water plan subbasins 03H and 031 Christina River Basin (Brandywine Creek and White Clay Creek watersheds) Chester, Delaware and Lancaster counties. 21 pp., Harrisburg, Pennsylvania

Richardson, A. J., and C. L. Wiegand (1977), Distinguishing vegetation from soil background information, Photogramm. Eng. Remote Sensing, 43(12), 1543–1551.

Scharf, P. C., J. P. Schmidt, N. R. Kitchen, K. a Sudduth, S. Y. Hong, J. a Lory, and J. G. Davis (2002), Remote sensing for nitrogen management, J. Soil Water Conserv. , 57 (6), 518–524.

Souza Jr., C. M., D. a Roberts, and A. L. Monteiro (2005), Multi-temporal analysis of degraded forests in the southern Brazilian Amazon, Earth Interact., 9(19), 1-25, doi:10.1175/EI132.1.

Stabile, M. C. ., and S. W. Searcy (2009), Validation of the soil line transformation technique, Trans. ASAE, 52(2), 633–640.

Suess, A., and J. Curtis (2006), Report: Value-added strategies for spent mushroom substrate in BC, prepared for British Columbia Mushroom Industry, 101 pp., Br. Columbia Minist. Agric. Lands., British Columbia, Canada

Taniguchi, K., K. Obata, and H. Yoshioka (2016), Soil isoline equations in the red–NIR reflectance subspace describe a heterogeneous canopy, J. Appl. Remote Sens., 10(1), 016013, doi:10.1117/1.JRS.10.016013.

Tesoriero, A. J., J. H. Duff, D. a. Saad, N. E. Spahr, and D. M. Wolock (2013), Vulnerability of streams to legacy nitrate sources, Environ. Sci. Technol., 47(8), 3623–3629, doi:10.1021/es305026x.

United States Census Bureau (2014), Cb_2014_us_state_5m, https://www.census.gov/geo/maps-data/, Philadelphia, Pennsylvania.

United States Department of Agriculture (n.d.), NAIP Imagery, Available from: http://www.fsa.usda.gov/programs-and-services/aerial-photography/imagery-programs/naip-imagery/ (Accessed 15 March 2015)

United States Department of Agriculture National Agricultural Statistics Service (2012), 2012 Census of Agriculture County Profile: Chester County, Pennsylvania, 2 pp. Washington, D.C.

United States Department of Agriculture (USDA), National Agricultural Statistics Service (NASS), Research and Development Division (RDD), Geospatial Information Branch (GIB), S. A. R. S. (SARS) (2012), 2011 Pennsylvania Cropland Data Layer, https://gdg.sc.egov.usda.gov/, Washington, D.C.

United States Geological Survey (2002), SPARROW decision support system- 2002 total nitrogen model for Northeast and Mid-Atlantic Regions (MRB1), Available from: http://cida.usgs.gov/sparrow/map.jsp?model=51 (Accessed 7 April 2016)

United States Geological Survey (2004), NHD Flowline- Delaware, www.pasda.psu.edu, Reston, Virginia

Unites States Geological Survey (2015a), Landsat Earth observation satellites fact sheet, 2013–2016.

United States Geological Survey (2015b), Product guide: Landsat 4-7 climate data record (DCR) - Surface Reflectance.

United States Geological Survey (2016), National Hydrography Dataset (NHD) Hydrologic Units (HUC) 12, http://opendata.firstmap.delaware.gov/, Reston, Virginia

United States Geological Survey (n.d.), Delaware: Surface-water resources, Water-Supply Paper 2400, Delaware, Baltimore, Maryland. http://md.water.usgs.gov/publications/wsp-2400/de-html.html#22 (Accessed 4 April 2016)

University of Delaware Water Resources Agency (n.d.) a, Red Clay Creek, Available from: http://delawarewatersheds.org/piedmont/red-clay-creek/ (Accessed 22 March 2016)

University of Delaware Water Resources Agency (n.d.) b, White Clay Creek, Available from: http://delawarewatersheds.org/piedmont/white-clay-creek/ (Accessed 22 March 2016)

University of Delaware Water Resources Agency (n.d.) c, White Clay Creek wild and scenic river program, Available from: http://www.wra.udel.edu/public-service/watershedmanagement/wccwildandscenicriver/ (Accessed 8 April 2016)

University of Delaware Water Resources Agency (n.d.) d, Christina Basin Clean Water Partnership organizational chart, Available from: http://www.wra.udel.edu/public-service/watershedmanagement/christinabasinpartnership/partnership/ (Accessed 5 April 2016)

Vicente-Serrano, S. M., X. Pons-Fernández, and J. M. Cuadrat-Prats (2004), Mapping soil moisture in the central Ebro river valley (northeast Spain) with Landsat and NOAA satellite imagery: a comparison with meteorological data, Int. J. Remote Sens., 25(20), 4325–4350.

Weber, L., Cole, P., Hautau, M., Oshins, C. (1997), Comparison of mushroom substrate and fertilizer as a nutrient source for corn, Mushroom News, Sci. Technol.

Wuest, P. (1983), Resources needed to farm the “Champignon,” Mycol. Soc. Am., *75*(2), 341–350.

Xu, D., and X. Guo (2013), A study of soil line simulation from Landsat images in mixed grassland, Remote Sens., 5(9), 4533–4550, doi:10.3390/rs5094533.

Yoshioka, H., T. Miura, J. a M. Demattê, K. Batchily, and A. R. Huete (2010), Soil line influences on two-band vegetation indices and vegetation isolines: A numerical study, Remote Sens., 2(2), 545–561, doi:10.3390/rs2020545.

Appendix A

PRELIMINARY RESULTS

A.1 Using a Supervised Classification and 1-m Resolution NAIP Imagery to Estimate the Spatial Distribution of Field-applied Mushroom Compost

In a preliminary analysis, we attempted to identify field-applied mushroom compost using multispectral high resolution imagery and using a simple supervised classification procedure. We expected the high resolution imagery to detect precise locations of compost application. We used 1 meter spatial resolution imagery from the National Agricultural Imagery Program (NAIP), collected in June and July of 2013. NAIP imagery is typically collected during the growing season when there is vegetation cover.

We performed a supervised classification on the NAIP imagery using ENVI version 4.8 (Exelis Visual Information Solutions, Boulder, Colorado). This process involved manually delineating training sites to help guide the computer-automated classification process. We selected training sites for five classes: forest, developed, agriculture, field-applied compost, and compost piles. We anticipated the areas with mushroom compost to possess a unique spectral response.

This preliminary analysis yielded a classification of compost application across the study area (Figure A.1). However, the results demonstrated that this classification lacked accuracy, because vegetation interfered with the spectral response of compost. NAIP imagery is collected during the leaf-on season, and therefore it was not suited to identify field applied compost to crop fields.

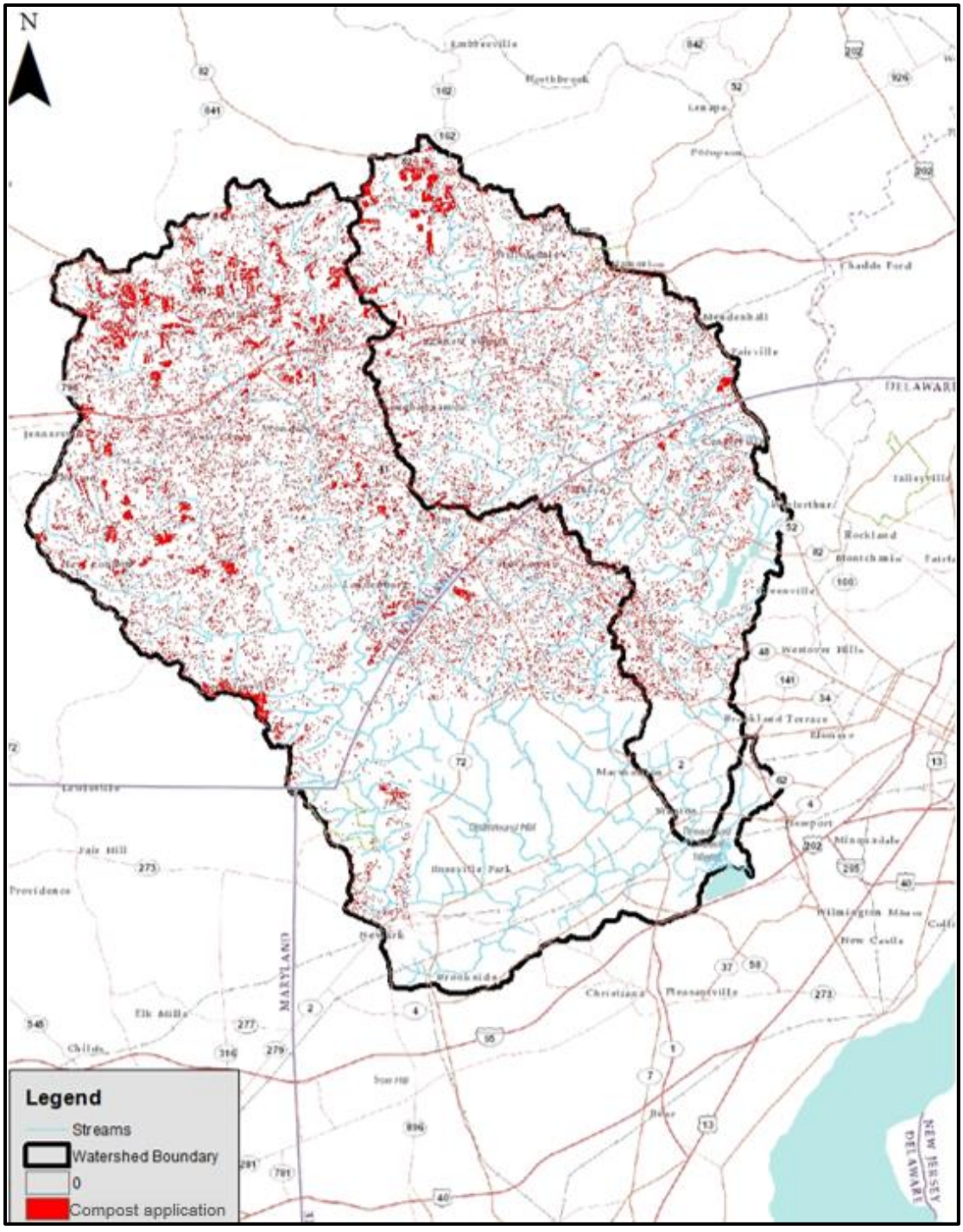

Figure A.1: Preliminary estimates of compost application in the White Clay Creek and Red Clay Creek Watersheds. This preliminary analysis uses high resolution NAIP imagery and supervised classification. We found that the estimates of this map are inaccurate, because of interference by vegetation.

A.2 Effect of Soil Type and Water Holding Capacity on Soil Line Calculations in Red-NIR Spectral Space

During preliminary analysis we initially divided the study area by soil type, because soil texture can affect the soil line. We used soil water holding capacity to classify different soil types. We used soil survey data obtained from SSURGO and distributed by ESRI. We divided the soils into two classes based on their water holding capacity of the first 20 centimeter of the soil columns: high soil water holding capacity (retain 4.5 centimeters of water, or more), and low soil water holding capacity (retain less than 4.5 centimeters of water).

We plotted the spectral responses of the two soil types in Red-NIR spectral space and calculated their soil lines. We found the two soil types had very similar spectral shapes (Figure A2.1), and their soil lines overlapped (Figure A2.2). Therefore, for the remainder of our study we did not consider differences in soil types, and used a single soil line instead.

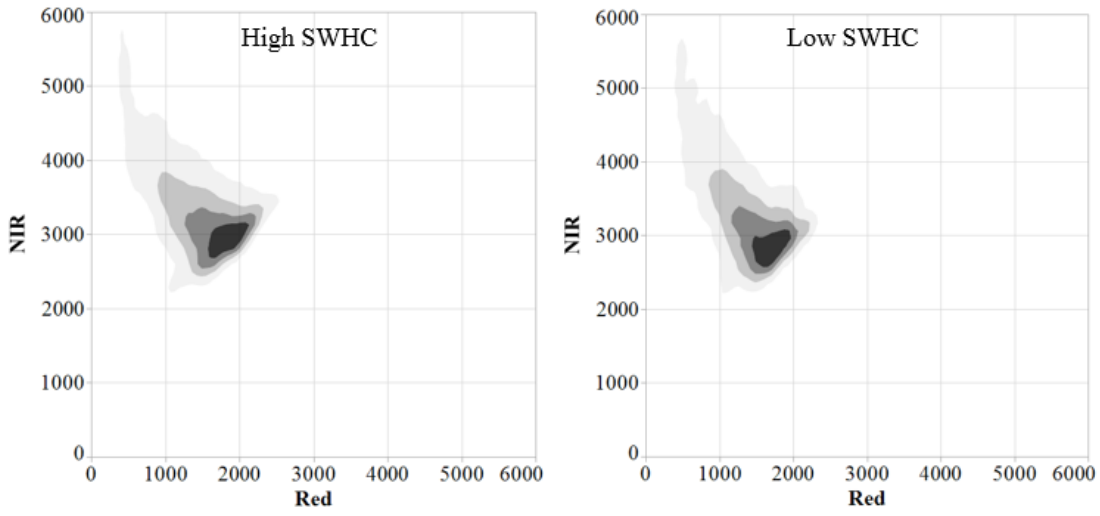

Figure A.2: Density graphs of two soil types (high and low SWHC) in Red-NIR spectral space.

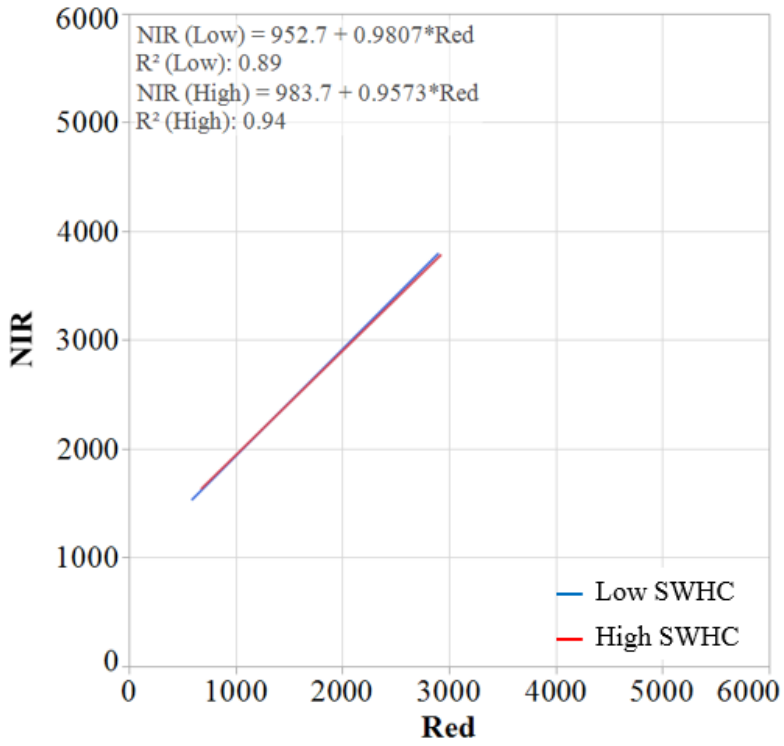

Figure A.3: Soil lines extracted for two soil types (high and low SWHC) within the study area.

Appendix B

COPYRIGHT PERMISSIONS

Permissions was obtained through email contact to use a table from Fidanza et al. (2010) and figure from Landschoot and McNitt (n.d.). The following pages include copyright permission with Journal of the American Society for Horticultural Science (Figure B.1) and Dr. Landschoot (Figure B.2).

Copyright permission
2 messages

Kelsey Moxey <kmoxey@udel.edu> Fri, Jul 1, 2016 at 12:15 PM
To: webmaster@ashs.org

Hello,

My name is Kelsey Moxey and I am a graduate student in Water Science and Policy at the University of Delaware. I am emailing to request permission to reprint a table from a publication in the Journal of HortTechnology. I could not find a copyright permission form from your ASHS website. What is the process to request permission for reprinting a figure for a master's thesis?

I am specifically interested reprinting Table 2 in:
Fidanza, M. a., D. L. Sanford, D. M. Beyer, and D. J. Aurentz (2010), Analysis of fresh mushroom compost, Hort technology, 20(2), 449–453.

Thank you for your time,

Kelsey

--
Kelsey A. Moxey

M.S. Candidate
Water Science and Policy
University of Delaware
205 Pearson Hall
Newark, Delaware 19716

Michael Neff <mwneff@ashs.org> Fri, Jul 1, 2016 at 12:27 PM
To: Kelsey Moxey <kmoxey@udel.edu>

Dear Kelsey,

Permission is hereby granted to reproduce the requested material. ASHS requires that appropriate credit be given to the author(s) and the publication from which the work is taken. Thank you for your support of the ASHS journals.

Best wishes on your thesis!

Michael Neff
Publisher, ASHS

Michael W. Neff
Executive Director
American Society for Horticultural Science
1018 Duke Street
Alexandria, VA 22314
mwneff@ashs.org
ashs.org
[Quoted text hidden]

Figure B.1: Email conversation requesting copyright permission from the Executive Director of the American Society for Horticultural Science.

Copyright Permission
2 messages

Kelsey Moxey <kmoxey@udel.edu> Wed, Jul 6, 2016 at 11:16 AM
To: pjl1@psu.edu, amcnitt@psu.edu

Hello Dr. Landschoot and Dr. McNitt,

My name is Kelsey Moxey, and I am a graduate student in the Water Science and Policy program at the University of Delaware. I am writing to the both of you today to request permission to use Figure 5 in your report titled "Using Spent Mushroom Substrate (mushroom soil) as a Soil Amendment to Improve Turf" for my master's thesis. Please let me know at your earliest convenience if using this figure is acceptable.

Thank you for your time,

Kelsey Moxey

--
Kelsey A. Moxey

M.S. Candidate
Water Science and Policy
University of Delaware
205 Pearson Hall
Newark, Delaware 19716

Peter Landschoot <pjl1@psu.edu> Wed, Jul 6, 2016 at 11:28 AM
To: Kelsey Moxey <kmoxey@udel.edu>
Cc: "amcnitt@psu.edu" <amcnitt@psu.edu>

Sure Kelsey.

Pete Landschoot

Sent from my iPhone
[Quoted text hidden]

Figure B.2: Email conversation requesting copyright permission from authors (Dr. Landschoot) of Pennsylvania State University.